Probing the Influence of Local Coordination Environment on Ligand Binding in Nickel Hydrogenase Model Complexes†

Mikyung Cha, Christine L. Gatlin, Susan C. Critchlow, and Julie A. Kovacs*

Department of Chemistry, University of Washington, Seattle, Washington 98195

Received February 19, 1992®

We report the synthesis and structure of three structurally-related mononuclear S-ligated Ni(II) complexes, 6-coordinate $[Ni(L_{S3N2})(MeCN)]^{2+}$ (**1**; $L_{S3N2} = (H_2NC_2H_4SC_2H_4)_2S$), 6-coordinate [Ni(BATES)Cl]$^+$ (**2**; BATES = $(H_2N\text{-}o\text{-}C_6H_4SC_2H_4)_2S$), and 5-coordinate $Ni(L_{S5})$ (**3**; $L_{S5} = (^-S\text{-}o\text{-}C_6H_4SC_2H_4)_2S$), which contain Ni in a S-rich environment possibly resembling that of the *active form* of nickel hydrogenases. Complex **1** crystallizes in the monoclinic space group $P2_1/n$ with $a = 19.036(2)$ Å, $b = 12.022(8)$ Å, $c = 24.953(4)$ Å, $\beta = 107.78(1)°$, and $Z = 4$. Complex **2** crystallizes in the space group $P\bar{1}$ with $a = 11.213(1)$ Å, $b = 13.482(2)$ Å, $c = 14.414(2)$ Å, $\alpha = 72.82(1)°$, $\beta = 89.862(9)°$, $\gamma = 69.396(9)°$, and $Z = 2$. Complex **3** crystallizes in the monoclinic space group $P2_1/c$ with $a = 10.759(2)$ Å, $b = 11.251(3)$ Å, $c = 14.198(1)$ Å, $\beta = 90.82(1)°$, and $Z = 4$. Structures **1–3** share a common trithioether ($S_{apical}(C_2H_4SR_{eq})_2$; $R_{eq} = C_2H_4NH_2$ (**1**), $C_6H_4NH_2$ (**2**), or $C_6H_4S^-$ (**3**)) "backbone" and possess either a "vacant" or a labile coordination site. These structures differ in terms of their molecular charge (2+ (**1**), 1+ (**2**), 0 (**3**)) and terminal ligating atoms. The amine-ligated complexes **1** and **2** have a higher affinity for axial ligands and are more reactive than the thiolate-ligated complex **3**. The Ni-bound MeCN solvent molecule of **1** is exchangeable and readily displaced by weaker coordinating solvents, as well as anionic ligands. X-ray structures of the most stable derivatives of **1**, $[Ni(L_{S3N2})(py)]^{2+}$ (**7**), $[Ni(L_{S3N2})(N_3)]^+$ (**8**), and $[Ni(L_{S3N2})(Cl)]^+$ (**9**), are presented, and structural parameters are compared for $[Ni(L_{S3N2})(L)]^{n+}$ ($n = 1, 2$; L = MeCN (**1**), py (**7**), N_3^- (**8**), Cl^- (**9**), and Br^- (**4**)). Reaction of **2** with $NaBH_4$ at –42 °C affords a thermally unstable species **10**, which behaves like a Ni–H in terms of its reactivity. Hydride derivative **10** will hydrogenate olefins (styrene and cyclohexene) and convert $CDCl_3$ to $CHDCl_2$. In contrast to the amine-ligated complexes, thiolate-ligated **3** is fairly unreactive with respect to binding axial ligands. The only ligand examined in this study which was strong enough to induce the spin-state change required in converting **3** to a 6-coordinate structure was pyridine. Implications that this observed decrease in reactivity, upon substitution of terminal amines with aromatic thiolates, has with respect to the probable structure of the Ni-binding site of hydrogenase is also discussed.

Research efforts in our group have been directed toward the design and synthesis of mononuclear Ni complexes which contain Ni in a S-rich environment resembling that of the reactive, reduced form of Ni hydrogenases (H_2-ases)[1-4] and which incorporate features designed to promote reactivity. The Ni site in H_2-ases catalyzes H^+/D_2 exchange, H_2 activation and oxidation, or, in some cases, H_2 evolution. Although the Ni sites do not appear to be identical for all H_2-ases, all of them are mononuclear, redox active,[4] and attached to the protein "backbone" via one to four S-containing residues (S_{cys} or S_{met}) and at least one N-containing residue.[5] When isolated, the enzyme is found in a partially oxidized inactive Ni(III) state. Full activity expression requires that the Ni site be reduced.[4b] Synthetic modeling studies have shown that Ni(III) can be made thermodynamically accessible by placing it in a thiolate-rich environment.[7a,c-e,j] EXAFS,[3,5,6] and EPR[2,4] studies indicate that the Ni ion in the inactive Ni(III) form of H_2-ase is probably located in an elongated octahedral environment. The reduced Ni ion appears to be 5-coordinate, on the bases of recent XANES,[3,6] MCD,[8] and magnetization studies[9] A critical question which relates to the function of Ni in H_2-ase

† In this paper, boldface numbers denoting chemical species may refer to either the cationic coordination sphere or the neutral salt.

* Abstract published in *Advance ACS Abstracts,* October 15, 1993.

(1) (a) Kovacs, J. A. In *Advances in Inorganic Biochemistry*; Eichhorn, G. L., Marzilli, L. G., Eds.; Prentice-Hall: Englewood Cliffs, NJ, 1993; Vol. 9, Chapter 5. (b) Hausinger, R. P. *Microbiol. Rev.* **1987**, *51*, 22. (c) Walsh, C. T.; Orme-Johnson, W. H. *Biochemistry* **1987**, *26*, 4901. (d) Salerno, J. C. In *The Bioinorganic Chemistry of Nickel*; Lancaster, J. R., Jr., Ed.; VCH: New York, 1988.

(2) (a) Fauque, G.; Peck, H. D., Jr.; Moura, J. J. G.; Huynh, B. H.; Berleir, Y.; DerVartanian, D. V.; Teixeira, M.; Przybyla, A. E.; Lespinat P. A.; Moura, I.; LeGall, J. *FEMS Microbiol. Rev.* **1988**, *54*, 299. (b) R. Cammack *Adv. Inorg. Chem.* **1988**, *32*, 297. (c) Moura, J. J. G.; Teixeira, M.; Moura, I. *Pure Appl. Chem.* **1989**, *61*, 915. (d) Cammack, R.; Fernandez, V. M.; Schneider, K. In *The Bioinorganic Chemistry of Nickel*; Lancaster, J. R., Jr., Ed.; VCH: New York, 1988; Chapter 8. (e) Moura, J. J. G.; Teixeira, M.; Moura, I.; LeGall, J. In *The Bioinorganic Chemistry of Nickel*; Lancaster, J. R., Jr., Ed.; VCH: New York, 1988; Chapter 9. (f) van der Zwaan, J. W.; Albracht, S. P. J.; Fontijn, R. D.; Slater, E. C. *FEBS Lett.* **1985**, *179*, 271. (g) Huynh, B. H.; Patil, D. S.; Moura, I.; Teixeira, M.; Moura, J. J. G.; DerVartanian, D. V; Czechowski, M. H.; Prickril, B. C.; Peck, H. D., Jr.; LeGall, J. *J. Biol. Chem.* **1987**, *262*, 795. (h) Kowal, A. T.; Zambrano, I. C.; Moura, I.; Moura, J. J. G.; LeGall, J.; Johnson, M. K. *Inorg. Chem.* **1988**, *27*, 1162.

(3) Maroney, M. J.; Colpas, G. J.; Bagyinka, C. *J. Am. Chem. Soc.* **1990**, *112*, 7067.

(4) (a) Moura, J. J. G.; Teixeira, M.; Moura, I.; Xavier, A. V.; LeGall, J. *J. Mol. Catal.* **1984**, *23*, 303. (b) Teixeira, M.; Moura, I.; Xavier, A. V.; Huynh, B. H.; DerVartanian, D. V; Peck, H. D., Jr.; LeGall, J.; Moura, J. J. G. *J. Biol. Chem.* **1985**, *260*, 8942.

(5) (a) Lindahl, P. A.; Kojima, N.; Hausinger, R. P.; Fox, J. A.; Teo, B. K.; Walsh, C. T.; Orme-Johnson, W. H. *J. Am. Chem. Soc.* **1984**, *106*, 3062. (b) Scott, R. A.; Wallin, S. A.; Czechowski, M.; DerVartanian, D. V.; LeGall, J.; Peck, H. D., Jr; Moura, I. *J. Am. Chem. Soc.* **1984**, *106*, 6864. (c) Chapman, A.; Cammack, R.; Hatchikian, C. E.; McCracken, J.; Peisach, J. *FEBS Lett.* **1988**, *242*, 134.

(6) Colpas, G. J.; Maroney, M. J.; Bagyinka, C.; Kumar, M.; Willis, W. S.; Suib, S. L.; Baidya, N.; Mascharak, P. K. *Inorg. Chem.* **1991**, *20*, 920.

(7) (a) Kruger, H.-J.; Peng, G.; Holm, R. H. *Inorg. Chem.* **1991**, *30*, 734. (b) Baidya, M.; Olmstead, M.; Mascharak, P. K. *Inorg. Chem.* **1991**, *30*, 929. (c) Fox, S.; Wang, Y.; Silver, A.; Millar, M. *J. Am. Chem. Soc.* **1990**, *112*, 3218. (d) Kruger, H.-J.; Holm, R. H. *Inorg. Chem.* **1989**, *28*, 1148. (e) Kruger, H.-J.; Holm, R. H. *J. Am. Chem. Soc.* **1990**, *112*, 2955. (f) Rosenfield, S. G.; Berends, H. P.; Gelmini, L.; Stephan, D. W.; Mascharak, P. K. *Inorg. Chem.* **1987**, *26*, 2792. (g) Mills, D. K.; Reibenspies, J. H.; Darensbourg, M. Y. *Inorg. Chem.* **1990**, *29*, 4364. (h) Kumar, M.; Colpas, G. J.; Day, R. O.; Maroney, M. *J. Am. Chem. Soc.* **1989**, *111*, 8323. (i) Kumar, M.; Day, R. O.; Colpas, G. J.; Maroney, M. J. *J. Am. Chem. Soc.* **1989**, *111*, 5974. (j) Kruger, H.-J.; Holm, R. H. *Inorg. Chem.* **1987**, *26*, 3647. (k) Snyder, B. S.; Rao, C. P.; Holm, R. H. *Aust. J. Chem.* **1986**, *39*, 963. (l) Yamamura, T.; Miyamae, H.; Katayama, Y.; Sasaki, Y. *Chem. Lett.* **1985**, 269.

(8) Kowal, Q. T.; Zambrano, I. C.; Moura, I.; Moura, J. J. G.; LeGall, J.; Johnson, M. K. *Inorg. Chem.* **1988**, *27*, 1162.

(9) Wang, C.-P.; Franco, R.; Moura, J. J. G.; Moura, I.; Day, E. P. *J. Biol. Chem.* **1992**, *267*, 7378.

0020-1669/93/1332-5868$04.00/0 © 1993 American Chemical Society

concerns the mechanism by which the reduced Ni ion activates or evolves H_2. ENDOR[10] and EPR[2f] studies suggest that dihydrogen activation occurs at the Ni site and may involve either a Ni–H or Ni(σ-H_2)[11] intermediate. H_2 cleavage appears to be heterolytic since H_2/D^+ exchange is observed. Most likely, this is assisted by a coordinated[12] or nearby base[13] (Ni-B: + H_2 → Ni(σ-H_2)-B: → Ni(H)--BH) and would require that there be either a vacant, or labile, site on the Ni ion and that the Ni ion have an affinity for binding substrates at this site.

The most common geometry for homoleptic Ni(II) thiolates is 4-coordinate square planar. Examples include $[Ni(bdt)_2]^{2-/-}$,[14] $[Ni(edt)_2]^{2-}$,[7k,15] and $[Ni(nbdt)_2]^{2-}$.[7c] In this environment, however, Ni(II) tends to be less reactive than it would be if it were in either a 6-coordinate octahedral or 5-coordinate environment. The reactivity of a square planar Ni(II) complex can be increased either by adding an electron, to form a Ni(I) species,[38] or by adding axial ligands. Empirical evidence indicates that, for square planar Ni(II) complexes (NiL_4) that bind axial ligands, once one axial ligand binds (to form $NiL_4(A_1)$), the second axial ligand will add spontaneously (to form $NiL_4(A_1)(A_2)$). It is rare, in fact, for the intermediate 5-coordinate species $NiL_4(A_1)$ to be observed.[16] Taking these observations into account, our group has been working with, and designing, sulfur-containing ligands with a "built-in" axial ligand. We have chosen to work with open-chain pentadentate ligands since they would favor either a 5-coordinate structure with a "vacant" site or a 6-coordinate structure with a unique labile site and would allow basic sites (for H_2 deprotonation) to be incorporated in the terminal positions. Herein we report the synthesis and structure of three structurally-related mononuclear S-ligated Ni(II) complexes, **1–3**, which possess either a vacant or a unique labile coordination site. Although the axial ligand affinity of Ni(II) has been thoroughly investigated in N- and/or O-rich environments,[17] very little has been reported for Ni(II) in a S-rich environment. By systematically altering the terminal ligating atoms, we have been able to probe the influence that local coordination environment can have on a Ni ion's propensity to bind axial ligands when it is in a sulfur-rich environment.

Experimental Section

General Methods. Unless noted otherwise, all reactions were carried out under nitrogen at room temperature using Schlenk-line or drybox techniques. Solvents were dried over calcium hydride (MeCN), sodium benzophenone (THF), phosphorus pentoxide ($CHCl_3$), and sodium methoxide (MeOH) and freshly distilled under nitrogen and degassed before use. Deuterated solvents MeCN-d_3 and DMSO-d_6 were purified by distillation from CaH_2 under reduced pressure and stored over 3-Å molecular sieves inside a drybox. DMF-d_7 and THF-d_8 were used as received.

Bis(triphenylphosphine)nickel(II) chloride, phosphorus tribromide, sodium borohydride, and bis(2-bromoethyl) sulfide were purchased from Aldrich and used as received. Tetrabutylammonium tetrafluoroborate was recrystallized from ethyl acetate/pentane (v/v, 10/1) three times before use. Hexaaquonickel tetrafluoroborate and sodium tetraphenylborate were purchased from Strem and used as received. *o*-Aminothiophenol was distilled at 60 °C under partial vacuum. Benzene-1,2-dithiol and bis(2-hydroxyethyl) sulfide were purchased from Fluka and used as received. NMR spectra were recorded on a Bruker AC-200, AF-300, or VXR-500 spectrometer. IR spectra were obtained using KBr pellets or Nujol mulls between KBr plates on a Perkin-Elmer 1600 FT-IR. A Hewlett-Packard Model 8450 spectrometer, interfaced to an IBM PC, was used to record UV/vis/near-IR spectra. GC/MS measurements were taken with a Kratos Profile HP3 spectrometer. Elemental analyses were performed by Galbraith Labs, Knoxville, TN. Magnetic susceptibilities in the solid state were measured with a Cahn 7600 Faraday balance equipped with a Cahn 4100 electrobalance. Magnetic susceptibilities in solution were determined by the Evans NMR method as modified for high-field NMR spectrometers containing superconducting solenoids.[18] Solvent susceptibilities[19] and diamagnetic corrections[20] were taken from tabulated values. Electrochemical measurements were made at ambient temperature using standard Princeton Applied Research instrumentation (PAR-273 potentiostat/galvanostat) with a glassy carbon working electrode, a platinum wire counter electrode, 0.1 M Bu_4NBF_4 supporting electrolyte, and a SCE reference electrode.

Preparation of Compounds. $[Ni(L_{S3N2})(MeCN)](BPh_4)_2$·MeCN (1). Complex **1** was prepared by combining 5.8 g (24 mmol) of pentadentate ligand[21] L_{S3N2} with 6.3 g (24 mmol) of $[Ni(H_2O)_6](SO_4)$ in 250 mL of H_2O, stirring for 2 h, and filtering to remove any unreacted ligand. Following solvent removal, the lavender residue was extracted into MeOH (~150 mL), and the extract was filtered to remove unreacted $[Ni(H_2O)_6](SO_4)$. The SO_4^{2-} anion was exchanged with BPh_4^- by adding 2.6 g (12.3 mmol) of $BaCl_2·2H_2O$ followed by 8.4 g (24.6 mmol) of $NaBPh_4$, stirring for 24 h, removing the MeOH solvent, extracting the resulting lavender solid into MeCN (3 × 100 mL), and filtering to remove NaCl and $BaSO_4$. Slow evaporation of the MeCN solvent afforded 4.9 g (20% yield) of lavender X-ray-quality crystals of **1**. Anal. Calcd for $C_{60}H_{66}N_4S_3B_2Ni$: C, 70.67; H, 6.57; N, 5.49; S, 9.43. Found: C, 69.98; H, 6.33; N, 5.70; S, 8.91. Absorption spectrum (MeCN): λ_{max} (ϵ_M) 349 (33), 530 (17), 884 (25), 960 (sh) nm. ^1H NMR (MeCN-d_3): δ 144 (b), 130.6 (b), 115.6 (b), 80.6 (b), 65.6 (b), 23.7 (b), –55 (b), –65 (b), –138 (b). μ_{eff}(MeCN) = 2.85 μ_B; μ_{eff}(solid; 24 °C) = 2.90 μ_B.

Bis(2-((2-aminophenyl)thio)ethyl) Sulfide (BATES). Na (390 mg, 16.9 mmol) was added to 100 mL of MeOH, followed by 1.81 mL (16.9 mmol) of *o*-aminothiophenol and 2.1 g (8.5 mmol) of bis(2-bromoethyl) sulfide.[22] The yellow solution was refluxed for 2 h, and then the MeOH was removed under vacuum. The resulting oily-yellow solid was extracted into $CHCl_3$, and the extract was filtered to remove NaBr. The filtrate solvent was removed under vacuum to yield the product (BATES = $(H_2N\text{-}o\text{-}C_6H_4SC_2H_4)_2S$) as a yellow oil. Yield: 2.6 g (99%). ^1H NMR ($CDCl_3$): δ 7.36 and 7.32 (d of d, 2H, ^2J = 1.5 Hz, ^3J = 7.5 Hz), 7.12 (d of t, 2H, ^2J = 1.5 Hz, ^3J = 7.1 Hz), 6.67 (d of d and t of t, 4H), 4.31 (b, 4H, NH_2), 2.80 (m, 4H), 2.65 (m, 4H). ^{13}C NMR ($CDCl_3$): δ 148.5, 136.2, 130.1, 118.4, 116.4, 114.9, 34.4, 31.6. FAB-MS: *m/z* 337 (M^+).

[Ni(BATES)Cl]BPh_4·MeCN (2). $[Ni(H_2O)_6]SO_4$ (1.1 g, 4.20 mmol) was added to the BATES ligand (1.4 g, 4.20 mmol) dissolved in 100 mL of degassed MeOH. The reaction mixture was stirred for 3 h, resulting in a light lavender solid and a light green solution. $BaCl_2·2H_2O$ (1.0 g, 4.20 mmol) and $NaBPh_4$ (2.9 g, 8.50 mmol) were then added, and the mixture was stirred for 1 day. The mixture was anaerobically filtered to afford a light green solution and light lavender-pink solid. The solid was extracted into MeCN, followed by filtering to remove a light green solid. The resulting lavender-blue filtrate was slowly concentrated until lavender microcrystals formed. The air-stable crystalline product was collected by filtration, washed with hexane, and dried under vacuum. Yield: 1.20 g (38%). ^1H NMR (MeCN-d_3): δ 23.44, 20.5, 10.04, 8.94, 7.27 (d), 6.99 (t), 6.84 (t). Absorption spectrum (MeCN): λ_{max} (ϵ_M) 362 (42), 578 (22), 920 (29), 1010 (sh) nm. Anal. Calcd for $NiClS_3N_3C_{42}H_{43}B$: C, 63.99; H, 5.40; N, 4.15; S, 12.66; Cl, 4.66. Found: C, 64.00; H, 5.39; N, 4.21; S, 11.36; Cl, 5.04. μ_{eff}(MeCN) = 3.06 μ_B, μ_{eff} = 3.18 μ_B (solid state).

$L_{S5\text{-}H2}$ ($L_{S5\text{-}H2}$ = $(HS\text{-}o\text{-}C_6H_4SC_2H_4)_2S$). $L_{S5\text{-}H2}$ was synthesized using a modification of a previously reported procedure.[23] Bis(2-bromoethyl)

(10) Fan, C.; Teixeira, M.; Moura, J.; Moura, I.; Huynh, B.-H.; LeGall, J.; Peck, H. D., Jr.; Hoffman, B. M. *J. Am. Chem. Soc.* **1991**, *113*, 20.
(11) (a) Crabtree, R. H. *Inorg. Chim. Acta* **1986**, *125*, L7. (b) Kubas, G. J. *Acc. Chem. Res.* **1988**, *21*, 120.
(12) Shoner, S. C.; Olmstead, M.; Kovacs, J. A. *Inorg. Chem.*, in press.
(13) Brothers, P. *Prog. Inorg. Chem.* **1981**, *28*, 1.
(14) (a) Baker-Hawkes, M. J.; Billig, E.; Gray, H. B. *J. Am. Chem. Soc.* **1966**, *88*, 4870. (b) Cha, M.; Sletten, J.; Critchlow, S. C., Kovacs, J. A. Submitted for publication in *Inorg. Chem.* (c) Sellmann, D.; Funfgelder, S.; Knoch, F.; Moll, M. *Z. Naturforsch., B: Chem. Sci.* **1991**, *46*, 1601.
(15) Baidya, N.; Mascharak, P. K.; Stephan, D. W.; Campagna, C. F. *Inorg. Chim. Acta* **1990**, *177*, 233.
(16) Sacconi, L. In *Transition-Metal Chemistry*; Carlin, R. L., Ed.; Dekker: New York, 1968; Vol. 4, p 199.
(17) Sacconi, L.; Mani, F.; Bencini, A. In *Comprehensive Coordination Chemistry*; Wilkinson, G., Gillard, R. D., McClevarty, J. A., Eds.; Pergamon: New York, 1987; Vol. 5.
(18) Live, D. H.; Cahn, S. I. *Anal. Chem.* **1970**, *42*, 79.
(19) Gerger, W.; Mayer, U.; Gutmann, V. *Monatsh. Chem.* **1977**, *108*, 417.
(20) O'Connor, C. J. *Prog. Inorg. Chem.* **1982**, *29*, 203.
(21) L_{S3N2} (L_{S3N2} = $(H_2NC_2H_4SC_2H_4)_2S$) was synthesized as previously described: Amundsen, A. R.; Whelan, J.; Bosnich, B. *J. Am. Chem. Soc.* **1977**, *99*, 6730.
(22) Bis(2-bromoethyl) sulfide (*Caution! Bis(2-bromoethyl) sulfide is a mustard gas analog. Avoid inhalation and skin contact!*) was synthesized using a modification of a previously reported method: Steinkopf, L. J.; Herod, J. *Ber. Dtsch. Chem.* **1920**, *53*, 1007.
(23) Sellmann, D.; Kleine-Kleffmann, U. *J. Organomet. Chem.* **1983**, *258*, 315.

sulfide (1.52 g (5 mmol)) was added to a MeOH solution containing 2 equiv of monodeprotonated 1,2-benzenedithiol (o-$C_6H_4(SH)(S^-)Na^+$, which was prepared by reaction of 1.2 mL (10 mmol) of o-$C_6H_5(SH)_2$ with 0.23 g (10 mmol) of Na in 50 mL of MeOH. Crude $L_{S5\text{-}H2}$ was obtained by removing the MeOH solvent under vacuum, extracting the product into CH_2Cl_2, filtering to remove NaBr, and evaporating the CH_2Cl_2 solvent. The resulting cloudy oil was then washed with MeOH to afford pure $L_{S5\text{-}H2}$ (FAB/MS (m/z): 370) as a clear yellow oil (1.66 g; 89.5% yield).

Ni(L_{S5}) (3). Complex **3** was prepared by adding 530 mg of NaOMe (9.5 mmol) to a THF solution (80 mL) containing 3.1 g (4.70 mmol) of $NiCl_2(PPh_3)_2$ and 1.7 g (4.7 mmol) of $L_{S5\text{-}H2}$, stirring overnight, and filtering to remove NaCl. Addition of ~5 mL of MeCN, followed by cooling (–20 °C; 4 days), afforded X-ray-quality single crystals (1.05 g, 50% yield of **3**). Anal. Calcd for $NiS_5C_{16}H_{16}$: C, 44.96; H, 3.77; S, 37.51. Found: C, 43.82; H, 3.65; S, 35.05. Absorption spectrum (CH_2Cl_2): λ_{max} (ϵ_M) 554 (140), 690 (88) nm. Absorption spectrum (DMF): λ_{max} (ϵ_M) 560 (99), 694 (66) nm.

[Ni(L_{S3N2})(py)](BPh_4)$_2$ (7). The pyridine-ligated derivative of **1** was obtained by dissolving **1** in neat pyridine, removing the solvent in vacuo, and then redissolving the isolated solid in neat pyridine. Air evaporation of the resulting pyridine solution afforded lavender microcrystalline samples of **7**.

[Ni(L_{S3N2})(N_3)](BPh_4)·MeCN (8). The azide derivative of **1** was obtained by reacting 1 equiv (31 mg, 0.48 mmol) of NaN_3 with **1** (48 mg, 0.48 mmol) in MeCN. The solution was cooled to –20 °C and filtered to remove $NaBPh_4$, and the filtrate was then concentrated and cooled to afford blue microcrystalline samples of compound **8**.

[Ni(L_{S3N2})(Cl)](BPh_4)·$(CH_3)_2C(O)$ (9). The chloride derivative of **1** was prepared using the same procedure used in the synthesis of MeCN-ligated **1**, except the BPh_4^- salt was extracted into acetone, as opposed to MeCN. Compound **9** was isolated by slow air evaporation of an acetone solution.

Reaction of 2 with $NaBH_4$. Reaction of **2** with $NaBH_4$ in MeCN-d_3 at –42 °C results in an immediate color change from lavender to blue and affords a thermally unstable species **10**, which decomposes upon warming (after 1 h at 17 °C) to form free ligand, Ni mirror, a black solid (nickel boride),[24] and H_2 gas (detected by ^{1}H NMR: δ 4.56). Samples of **10** were prepared by addition of a slurry of $NaBH_4$ (200 μL of a 44 mM MeCN-d_3 slurry) to a cooled (–42 °C) MeCN-d_3 (500 μL) solution of **2** (4.5 mg (6 μmol)) in an NMR tube. The tube was agitated to induce mixing, and the solution became homogeneous within 15 min.

Reaction of 2 with $NaBH_4$ + Olefins. Styrene (0.7 μL (6.5 μmol)) was injected into a sample of **10** in MeCN-d_3 prepared as described above. After 1.5 h at –42 °C, followed by warming to room temperature, 4.88 μmol (75%) of ethylbenzene (δ 2.605 (q, J = 7.6 Hz), 1.194 (t, J = 7.6 Hz), 7.28 (m), 7.26 (m), 6.86 (m)) was detected by ^{1}H NMR. Cyclohexene (0.6 μL (6.0 μmol)) was injected into a sample of **10** in MeCN-d_3 prepared as described above. After 3.0 h at –42 °C, followed by warming to room temperature, 3.74 μmol (62%) of cyclohexane (δ 1.43 (s)) was detected by ^{1}H NMR.

Reaction of 2 with $NaBH_4$ + $CDCl_3$. $CDCl_3$ (0.5 μL (6.2 μmol)) was injected into a sample of **10** in MeCN-d_3 prepared as described above. After 10 min at –4.2 °C, followed by warming to room temperature, 3.3 μmol (53%) of $CHDCl_2$ (δ 5.416 (t, J = 1.16 Hz)) was detected by ^{1}H NMR.

X-ray Structure Determinations of [Ni(L_{S3N2})(MeCN)](BPh_4)$_2$·MeCN (1), [Ni(BATES)(Cl)]BPh_4·MeCN (2), Ni(L_{S5}) (3), [Ni(L_{S3N2})(py)](BPh_4)$_2$ (7), [Ni(L_{S3N2})(N_3)](BPh_4)·MeCN (8), and [Ni(L_{S3N2})(Cl)](BPh_4)·$(CH_3)_2C(O)$ (9). Lavender single crystals of **1**, **7**, and **9** were obtained by air evaporation of CH_3CN, pyridine, and acetone solutions, respectively. Lavender X-ray-quality crystals of **2** were obtained by layering diethyl ether on top of a concentrated MeCN solution of **2**. Black single crystals of compound **3** were obtained by cooling a THF/MeCN (16/1) solution to –20 °C. Blue single crystals of **8** were obtained by slowly cooling a MeCN solution to –20 °C. Suitable crystals of **1** and **7**–**9** were mounted on glass fibers with epoxy. Crystals of **2** and **3** were mounted in glass capillaries whose sides were coated with Apiezon L grease, and the capillaries were flame-sealed under a dinitrogen atmosphere. X-ray crystallographic studies were done using an Enraf-Nonius CAD4 diffractometer and graphite-monochromated Mo Kα (λ = 0.710 73 Å) radiation at ambient temperature. X-ray data collection parameters are summarized in Table I for compounds **1**-**3** and in Table VIII for compounds **7**-**9**.

Table I. Crystal Data for [Ni(L_{S3N2})(MeCN)](BPh_4)$_2$·MeCN (**1**), [Ni(BATES)Cl](BPh_4)·MeCN (**2**), and Ni(L_{S5}) (**3**)

	1	**2**	**3**
formula	$NiS_3N_4C_{60}H_{66}B_2$	$NiClS_3N_3C_{42}H_{43}B$	$NiS_5C_{16}H_{16}$
fw	1019.17	791.00	427.34
unit cell[a]	monoclinic	triclinic	monoclinic
a, Å	19.036(2)	11.213(1)	10.759(2)
b, Å	12.022(8)	13.482(2)	11.251(3)
c, Å	24.953(4)	14.414(2)	14.198(1)
α, deg		72.82(1)	
β, deg	107.78(1)	89.862(9)	90.818(10)
γ, deg		69.396(9)	
V, Å^3	5438(2)	1945.8(5)	1718.4(6)
Z	4	2	4
ρ_{calc}, g/cm^3	1.247	1.350	1.652
space group	$P2_1/n$	$P\bar{1}$	$P2_1/c$
μ, cm^{-1}	5.1[b]	NA[c]	NA[c]
transm factors	1.000–0.765	NA[c]	NA[c]
R	0.048[d]	0.055[d]	0.044[e]
R_w	0.061	0.057	0.047
GOF	1.56	1.64	1.19

[a] In all cases: Mo Kα (λ = 0.710 73 Å) radiation; graphite monochromator; 24 °C. [b] An empirical absorption correction was applied. [c] No absorption correction was applied. [d] $R = \sum\|F_o\| - \|F_c\|$; $R_w = [\sum w(\|F_o\| - \|F_c\|)^2/\sum wF_o^2]^{1/2}$, where $w^{-1} = [\sigma_{count}^2 + (0.05F^2)^2]/4F^2$. [e] $R = \sum\|F_o\| - \|F_c\|$; $R_w = [\sum w(\|F_o\| - \|F_c\|)^2/\sum wF_o^2]^{1/2}$, where $w^{-1} = [\sigma_{count}^2 + (0.04F^2)^2]/4F^2$.

Cell constants and orientation matrices were obtained by least-squares refinement using the ranges 33° < 2θ < 39° for **1**, 28° < 2θ <36° for **2**, 29° < 2θ < 37° for **3**, 21° < 2θ < 28° for **7**, 22° < 2θ < 31° for **8**, and 30° < 2θ < 38° for **9**. The systematic absences $h0l$ ($h + l = 2n + 1$) and $0k0$ ($k = 2n + 1$) uniquely define the space group of **1**, **7**, and **9** as $P2_1/n$. The space group of **2** was determined to be $P\bar{1}$ by intensity statistics, and subsequent solution and refinement of the structure confirmed this space group. The systematic absences $h0l$ ($l = 2n+1$) and $0k0$ ($k = 2n+1$) uniquely define the space group of **3** and **8** as $P2_1/c$. An empirical absorption correction, based on a set of ψ scans, was applied for **1** and **8**, while no absorption correction was applied for **2**, **3**, **7**, and **9**. Three standard reflections examined after every 200 reflections showed no signs of decay for **3**, 2.1% decay for **1**, 11.5% decay for **2**, 1.7% decay for **7**, 2.3% decay for **8**, and 16.1% decay for **9**; a linear decay correction was applied to the data set for **2**. Heavy-atom positions were determined using a Patterson map for **1**, **2**, and **8** and the SHELX-86 direct-methods structure package for **3**, **7**, and **9**. The remaining non-hydrogen atoms were located from successive difference Fourier syntheses. All calculations were performed on a Micro-VAX computer using the SDP/VAX program supplied by the Enraf-Nonius Corp. Scattering factors were taken from a standard source.[25] Hydrogen atoms were fixed in calculated positions confirmed by a difference map. The 6142, 3803, 1732, 3255, 2081, and 3652 reflections with $I > 3\sigma(I)$ were used in the refinements of **1**–**3** and **7**–**9**, respectively. The final cycle of full-matrix least-squares refinement of **1**, **2**, **3**, and **8** with 631, 445, 200, and 391 parameters, respectively, converged with R factors (R (R_w)) of 0.048 (0.061), 0.055 (0.057), 0.044 (0.047), and 0.073 (0.084), respectively. Due to the disorder of an unidentified solvent in **7** and presence of a disordered $(CH_3)_2CO$ solvate molecule which could not be modeled for **9**, the final cycle of full-matrix least-squares refinement did not converge (R (R_w) = 0.121 (0.153) for **7** and 0.087 (0.115) for **9**). Positional parameters for compounds **1**–**3** are given in Tables II–IV, respectively, and those for compounds **7**–**9** are given in Tables IX–XI, respectively. Selected bond distances and angles are summarized in Tables V and XII.

Results and Discussion

Syntheses of 1–3. The structurally-related, mononuclear, sulfur-ligated Ni(II) complexes [Ni(L_{S3N2})(MeCN)](BPh_4)$_2$ (**1**), [Ni(BATES)Cl]BPh_4 (**2**), and Ni(L_{S5}) (**3**) were synthesized according to reactions 1–3 of Figure 1, respectively. The amine–trithioether ligand L_{S3N2} was synthesized as described previously by Bosnich and co-workers.[21] The amine–trithioether ligand BATES was synthesized from o-aminothiophenol and bis(2-bromoethyl) sulfide in essentially quantitative yields. Soluble salts of the cationic L_{S3N2}- and BATES-ligated complexes were

(24) Ganem, B.; Osby, J. O. *Chem. Rev.* **1986**, *86*, 763.

(25) Cromer, D. T.; Waber, J. T. *International Tables for X-ray Crystallography*; Kynoch: Birmingham, England, 1974; Vol. IV.

Table II. Selected Positional Parameters for $[Ni(L_{S3N2})(MeCN)](BPh_4)_2 \cdot MeCN$ (**1**)

atom	*x*	*y*	*z*
Ni	0.30876(2)	0.26128(4)	0.09691(2)
S(1)	0.26475(6)	0.07032(9)	0.07838(4)
S(2)	0.18541(5)	0.30443(10)	0.09836(4)
S(3)	0.27118(6)	0.33067(9)	0.00195(4)
N(1)	0.3489(2)	0.2125(3)	0.18060(12)
N(2)	0.3578(2)	0.4180(3)	0.11817(13)
N(3)	0.4038(2)	0.2010(3)	0.08260(13)
C(1)	0.3198(2)	0.1057(4)	0.1934(2)
C(2)	0.3161(2)	0.0206(4)	0.1483(2)
C(3)	0.1728(2)	0.0773(4)	0.0833(2)
C(4)	0.1349(2)	0.1835(4)	0.0594(2)
C(5)	0.1609(2)	0.4135(4)	0.0453(2)
C(6)	0.1807(2)	0.3895(4)	−0.0074(2)
C(7)	0.3298(3)	0.4511(4)	0.0166(2)
C(8)	0.3493(4)	0.4951(5)	0.0724(2)
C(9)	0.4486(2)	0.1530(3)	0.0734(2)
C(10)	0.5060(3)	0.0901(5)	0.0605(2)

Table III. Selected Positional Parameters for $[Ni(BATES)Cl](BPh_4) \cdot MeCN$ (**2**)

atom	*x*	*y*	*z*
Ni	0.12679(7)	0.05395(6)	0.31791(6)
Cl	0.16997(15)	−0.00358(13)	0.49122(11)
S(1)	0.23143(15)	0.18448(14)	0.30714(13)
S(2)	0.11748(16)	0.11280(15)	0.13939(13)
S(3)	0.3049(2)	−0.1068(2)	0.3084(2)
N(1)	−0.0395(5)	0.1830(4)	0.3264(4)
N(2)	0.0251(4)	−0.0528(4)	0.3350(4)
C(1)	−0.0271(6)	0.2873(5)	0.3208(4)
C(2)	−0.1339(7)	0.3770(5)	0.3243(5)
C(3)	−0.1237(8)	0.4779(6)	0.3185(5)
C(4)	−0.0040(9)	0.4878(5)	0.3118(5)
C(5)	0.1030(7)	0.3995(5)	0.3091(5)
C(6)	0.0914(6)	0.2985(5)	0.3126(4)
C(7)	0.2658(6)	0.2260(5)	0.1807(5)
C(8)	0.1642(7)	0.2333(6)	0.1107(5)
C(9)	0.2604(9)	0.0104(6)	0.1150(6)
C(10)	0.2875(10)	−0.0997(8)	0.1789(6)
C(11)	0.2289(8)	−0.2036(6)	0.3596(5)
C(12)	0.3043(10)	−0.3190(7)	0.3915(6)
C(13)	0.2402(11)	−0.3933(6)	0.4313(7)
C(14)	0.1130(9)	−0.3581(6)	0.4393(6)
C(15)	0.0412(8)	−0.2472(5)	0.4084(5)
C(16)	0.0994(7)	−0.1697(5)	0.3678(4)

Table IV. Positional Parameters for $Ni(L_{S5})$ (**3**)

atom	*x*	*y*	*z*
Ni	0.62972(8)	0.17715(7)	0.27893(6)
S(1)	0.7896(2)	0.0785(2)	0.3387(1)
S(2)	0.7602(2)	0.2734(2)	0.1874(1)
S(3)	0.5656(2)	0.0634(2)	0.1150(1)
S(4)	0.4707(2)	0.2961(1)	0.2517(1)
S(5)	0.5226(2)	0.0794(2)	0.3831(1)
C(1)	0.9015(6)	0.0891(6)	0.2506(4)
C(2)	1.0032(7)	0.0128(7)	0.2487(5)
C(3)	1.0892(6)	0.0215(7)	0.1770(6)
C(4)	1.0749(7)	0.1048(8)	0.1065(6)
C(5)	0.9756(6)	0.1836(7)	0.1087(5)
C(6)	0.8873(6)	0.1734(6)	0.1791(4)
C(7)	0.6544(6)	0.1496(7)	0.0332(5)
C(8)	0.6987(6)	0.2712(6)	0.0679(5)
C(9)	0.4148(6)	0.1318(7)	0.1081(4)
C(10)	0.4065(6)	0.2615(7)	0.1356(5)
C(11)	0.3498(6)	0.2413(6)	0.3234(4)
C(12)	0.2343(7)	0.2964(6)	0.3225(5)
C(13)	0.1405(6)	0.2531(7)	0.3777(5)
C(14)	0.1645(6)	0.1541(7)	0.4349(5)
C(15)	0.2792(6)	0.1024(6)	0.4385(4)
C(16)	0.3749(6)	0.1455(6)	0.3816(4)

prepared using BPh_4^- anions. The chloride ion of **2** was extracted from the $BaCl_2$ used in the anion-exchange reaction. The dithiolate ligand L_{S5} was taken from the literature,[23] and complex **3** was prepared using a modification of a previously described method.[26]

Table V. Selected Bond Distances (Å) and Angles (deg) for Compounds **1–3**

	$[Ni(L_{S3N2})(MeCN)](BPh_4)_2 \cdot MeCN$ (**1**)		
Ni–S(1)	2.439(1)	S(2)–C(5)	1.821(4)
Ni–S(2)	2.4158(9)	S(3)–C(6)	1.810(3)
Ni–S(3)	2.4057(9)	S(3)–C(7)	1.797(4)
Ni–N(1)	2.077(2)	N(1)–C(1)	1.471(4)
Ni–N(2)	2.097(3)	N(2)–C(8)	1.441(5)
Ni–N(3)	2.078(3)	N(3)–C(9)	1.111(4)
S(1)–C(2)	1.820(3)	C(9)–C(10)	1.444(5)
S(1)–C(3)	1.793(4)	C(7)–C(8)	1.429(6)
S(2)–C(4)	1.847(4)	C(1)–C(2)	1.508(5)
N(3)–Ni–S(1)	84.60(9)	S(3)–Ni–N(2)	85.02(8)
N(3)–Ni–S(2)	168.08(9)	N(1)–Ni–N(2)	90.0(1)
N(3)–Ni–S(3)	87.94(8)	Ni–S(1)–C(2)	94.3(1)
N(3)–Ni–N(1)	90.1(1)	Ni–N(3)–C(9)	168.7(3)
N(3)–Ni–N(2)	90.7(1)	Ni–S(1)–C(3)	103.2(3)
S(1)–Ni–S(2)	85.74(3)	C(2)–S(1)–C(3)	101.5(2)
S(1)–Ni–S(3)	99.09(3)	Ni–S(2)–C(5)	100.3(1)
S(1)–Ni–N(1)	85.65(7)	Ni–S(2)–C(4)	100.1(1)
S(1)–Ni–N(2)	173.64(8)	C(4)–S(2)–C(5)	102.0(2)
S(2)–Ni–N(1)	96.09(7)	Ni–S(3)–C(6)	104.3(1)
S(2)–Ni–N(2)	99.40(8)	Ni–S(3)–C(7)	95.7(1)
S(2)–Ni–S(3)	86.69(3)	C(6)–S(3)–C(7)	102.7(2)
S(3)–Ni–N(1)	174.68(7)	N(3)–C(9)–C(10)	178.9(4)
	$[Ni(BATES)(Cl)]BPh_4 \cdot MeCN$ (**2**)		
Ni–S(1)	2.402(2)	S(2)–C(9)	1.808(8)
Ni–S(2)	2.455(2)	S(3)–C(10)	1.858(8)
Ni–S(3)	2.409(2)	S(3)–C(11)	1.766(7)
Ni–N(1)	2.082(4)	N(1)–C(1)	1.440(6)
Ni–N(2)	2.085(4)	N(2)–C(16)	1.443(7)
Ni–Cl	2.409(2)	C(1)–C(6)	1.384(7)
S(1)–C(6)	1.788(6)	C(7)–C(8)	1.521(8)
S(1)–C(7)	1.805(6)	C(9)–C(10)	1.43(1)
S(2)–C(8)	1.808(8)	C(11)–C(16)	1.370(8)
Cl–Ni–S(1)	87.18(5)	S(3)–Ni–N(1)	173.8(1)
Cl–Ni–S(2)	170.90(6)	S(3)–Ni–N(2)	83.1(1)
Cl–Ni–S(3)	89.09(6)	N(1)–Ni–N(2)	90.8(2)
Cl–Ni–N(1)	91.6(1)	Ni–S(1)–C(6)	96.7(2)
Cl–Ni–N(2)	90.2(1)	Ni–S(1)–C(7)	104.6(2)
S(1)–Ni–S(2)	86.13(6)	C(6)–S(1)–C(7)	101.5(3)
S(1)–Ni–S(3)	101.01(6)	Ni–S(2)–C(8)	102.8(2)
S(1)–Ni–N(1)	85.1(1)	Ni–S(2)–C(9)	101.5(2)
S(1)–Ni–N(2)	175.1(1)	C(8)–S(2)–C(9)	101.4(3)
S(2)–Ni–N(1)	94.0(1)	Ni–S(3)–C(10)	101.1(3)
S(2)–Ni–N(2)	96.9(1)	Ni–S(3)–C(11)	95.7(2)
S(2)–Ni–S(3)	86.15(6)	C(10)–S(3)–C(11)	98.0(3)
	$Ni(L_{S5})$ (**3**)		
Ni–S(1)	2.201(2)	S(3)–C(9)	1.796(7)
Ni–S(2)	2.219(2)	S(4)–C(10)	1.820(7)
Ni–S(3)	2.747(2)	S(4)–C(11)	1.774(6)
Ni–S(4)	2.204(2)	S(5)–C(16)	1.754(6)
Ni–S(5)	2.176(2)	C(1)–C(6)	1.395(8)
S(1)–C(1)	1.753(6)	C(7)–C(8)	1.528(9)
S(2)–C(6)	1.776(6)	C(9)–C(10)	1.514(9)
S(2)–C(8)	1.812(7)	C(11)–C(16)	1.383(8)
S(3)–C(7)	1.799(7)		
S(1)–Ni–S(2)	88.48(7)	Ni–S(2)–C(6)	102.9(2)
S(1)–Ni–S(3)	105.90(7)	Ni–S(2)–C(8)	108.8(2)
S(1)–Ni–S(4)	167.14(7)	Ni–S(5)–C(16)	105.4(2)
S(1)–Ni–S(5)	84.69(7)	Ni–S(3)–C(7)	99.8(2)
S(2)–Ni–S(3)	82.89(6)	Ni–S(3)–C(9)	93.5(2)
S(2)–Ni–S(4)	95.29(7)	C(7)–S(3)–C(9)	102.8(3)
S(2)–Ni–S(5)	172.42(7)	Ni–S(4)–C(10)	108.5(2)
S(3)–Ni–S(4)	86.80(6)	Ni–S(4)–C(11)	105.0(2)
S(3)–Ni–S(5)	102.12(6)	C(10)–S(4)–C(11)	100.0(3)
S(4)–Ni–S(5)	90.70(6)	C(6)–S(2)–C(8)	101.5(3)
Ni–S(1)–C(1)	103.6(2)		

Structures of 1–3. ORTEP diagrams of dicationic **1**, monocationic **2**, and neutral **3** are shown in Figure 2. Selected interatomic distances and angles are collected in Table V. The X-ray structures of **1** and **2** demonstrate that complexation of Ni(II) respectively by the pentadentate ligands L_{S3N2} and BATES,

(26) Sellmann, D.; Funfgelder, S.; Pohlmann, G.; Knoch, F.; Moll, M. *Inorg. Chem.* **1990**, *29*, 4772.

Table VI. Electronic Spectral Properties of $[Ni(L_{S3N2})(MeCN)](BPh_4)_2$ (**1**), Ni(BATES)Cl](BPh$_4$) (**2**), and $Ni(L_{S5})$ (**3**)

complex	solvent	λ_{max}, nm (ϵ_M)			
1	MeCN	349 (33)	528 (17)	878 (25)	950 (sh)
1	acetone	361 (75)	564 (46)	922 (sh)	1012 (31)
1	DMF	366 (26)	558 (13)	922 (sh)	1000 (30)
2	MeCN	362 (42)	578 (22)	920 (29)	1010 (sh)
2	acetone	360 (40)	580 (25)	920 (31)	1010 (sh)
3	CH_2Cl_2		554 (140)	690 (88)	
3	DMF		560 (99)	694 (66)	
3	THF		554 (125)	686 (70)	
3	py (343 K)		566 (109)	670 (sh)	970 (24)
3	py (323 K)		574 (93)	670 (sh)	970 (26)
3	py (303 K)		586 (79)	680 (sh)	970 (30)
3	py (283 K)		600 (74)		970 (37)

Table VII. Variable-Temperature ^{1}H NMR Data for $Ni(L_{S5})$ (**3**) in Neat py-d_5

T, K	δ, ppm vs TMS			
248	42.0	29.8	25.5	16.1
258	38.0	27.2	23.3	15.4
268	34.5	24.8	21.2	14.0
278	31.8	23.0	19.9	13.1
288	27.5	20.8	17.7	11.9
298	24.6	18.4	16.0	11.0
308	21.5	16.4	14.5	10.2
318	19.4	14.9	13.3	9.5
328	17.1	13.5	12.2	9.0
338	14.9	12.0	10.9	8.4
358	13.8	10.8	9.8	7.9

Table VIII. Crystal Data for $[Ni(L_{S3N2})(py)](BPh_4)_2$·solv[f] (**7**), $[Ni(L_{S3N2})(N_3)](BPh_4)$·MeCN (**8**), and $[Ni(L_{S3N2})(Cl)](BPh_4)$·$(CH_3)_2C(O)$ (**9**)

	7	**8**	**9**
formula	$NiN_3S_3C_{61}H_{65}B_2$	$NiS_3N_6C_{34}H_{43}B$	$NiClS_3ON_2C_{35}H_{46}B$
fw	1016.74	701.48	711.94
unit cell[a]	monoclinic	monoclinic	monoclinic
a, Å	11.207(6)	11.556(19)	11.573(7)
b, Å	34.635(12)	13.132(3)	13.085(2)
c, Å	14.855(3)	23.000(3)	23.884(9)
β, deg	93.41(3)	100.301(13)	100.59(4)
V, Å^3	5756(5)	3434(2)	3555(2)
Z	4	4	4
ρ_{calc}, g/cm^3	1.175	1.357	1.329
space group	$P2_1/n$	$P2_1/c$	$P2_1/n$
μ, cm^{-1}	NA[c]	7.74[b]	NA[c]
transm factors	NA[c]	1.000–0.898[b]	NA[c]
R	0.121[d]	0.073[e]	0.087[e]
R_w	0.153	0.084	0.115
GOF	2.72	1.50	2.25

[a] In all cases: Mo K$\bar{\alpha}$ (λ = 0.710 73 Å) radiation; graphite monochromator; 24 °C. [b] An empirical absorption correction was applied. [c] No absorption correction was applied. [d] $R = \sum\|F_o\| - \|F_c\|; R_w = [\sum w(\|F_o\| - \|F_c\|)^2/\sum wF_o^2]^{1/2}$, where $w^{-1} = [\sigma_{count}^2 + (0.06F^2)^2]/4F^2$. [e] $R = \sum\|F_o\| - \|F_c\|; R_w = [\sum w(\|F_o\| - \|F_c\|)^2/\sum wF_o^2]^{1/2}$, where $w^{-1} = [\sigma_{count}^2 + (0.07F^2)^2]/4F^2$. [f] Six atoms of one or two solvate molecules were found but could not be modeled as a specific molecule (MeCN or py).

which contain terminal amines, affords 6-coordinate mononuclear structures, with either a MeCN solvent molecule (**1**) or a chloride ion (**2**) in the sixth position. In contrast, the X-ray structure of **3** demonstrates that the pentadentate ligand, L_{S5}, which contains terminal thiolates, affords a 5-coordinate mononuclear structure.

Complex **1** is distorted from C_s symmetry by an elongation of the trans Ni–S(1) and Ni–N(2) bonds; Ni–S(1) = 2.439(1) Å vs Ni–S(3) = 2.4057(9) Å, and Ni–N(2) = 2.097(3) Å vs Ni–N(1) = 2.077(2) Å. This contrasts with the structure of the Br-ligated derivative of **1**, $[Ni(L_{S3N2})(Br)](Br)$ (**4**),[27] which has a crystallographic mirror plane that imposes C_s symmetry. In complex **2** the mirror-related distances under C_s symmetry are within 3σ of one another; Ni–S(1) = 2.402(2) Å vs Ni–S(3) = 2.409(2) Å, and Ni–N(2) = 2.085(4) Å vs Ni–N(1) = 2.082(4) Å. The benzene ring attached to S(3) and N(2) in structure **2** is, however, tilted away from the NiN(1)S(1)S(3)N(2) plane by 21.9°. The Ni ions of both **1** and **2** sit in their N(1)S(1)S(3)N(2) planes with displacements of only 0.07 and 0.02 Å toward S(2), respectively. The mean Ni–N(amine) distances in **1** (Ni–N = 2.09(1) Å) and **2** (Ni–N = 2.084(2) Å) fall in the normal range for 6-coordinate Ni(II) complexes. The "apical" Ni–S(2)

Table IX. Selected Positional Parameters for $[Ni(L_{S3N2})(py)](BPh_4)_2$ (**7**)

atom	x	y	z
Ni	0.8005(2)	0.15456(8)	0.9097(2)
S(1)	0.9919(4)	0.1766(2)	0.9810(4)
S(2)	0.7200(5)	0.1629(2)	1.0591(4)
S(3)	0.8217(5)	0.0867(2)	0.9488(4)
N(1)	0.773(1)	0.2131(5)	0.881(1)
N(2)	0.639(1)	0.1394(5)	0.847(1)
N(3)	0.883(1)	0.1459(4)	0.7867(9)
C(1)	0.890(2)	0.2332(5)	0.874(1)
C(2)	0.973(2)	0.2268(6)	0.959(1)
C(3)	0.968(2)	0.1750(7)	1.100(1)
C(4)	0.841(2)	0.1822(7)	1.124(1)
C(5)	0.715(2)	0.1154(6)	1.105(1)
C(6)	0.807(2)	0.0873(5)	1.070(1)
C(7)	0.675(2)	0.0738(8)	0.906(2)
C(8)	0.586(2)	0.1063(7)	0.889(2)
C(11)	0.858(2)	0.1666(7)	0.718(1)
C(12)	0.915(2)	0.1643(8)	0.635(1)
C(13)	1.016(2)	0.1424(7)	0.634(1)
C(14)	1.044(2)	0.1208(7)	0.705(2)
C(15)	0.984(2)	0.1240(6)	0.787(1)

Table X. Selected Positional Parameters for $[Ni(L_{S3N2})(N_3)](BPh_4)$·MeCN (**8**)

atom	x	y	z
Ni	0.7456(1)	0.0405(1)	0.08315(7)
S(1)	0.5732(3)	–0.0645(3)	0.0590(2)
S(2)	0.6477(3)	0.1130(4)	0.1612(2)
S(3)	0.6712(3)	0.1902(3)	0.0269(2)
N(1)	0.823(1)	–0.0849(8)	0.1346(5)
N(2)	0.9025(8)	0.1221(8)	0.1063(5)
N(3)	0.7938(9)	–0.0181(9)	0.0075(4)
N(4)	0.8742(8)	–0.0703(8)	0.0042(4)
N(5)	0.9496(9)	–0.1234(9)	–0.0022(5)
N(6)	0.167(1)	0.525(1)	0.0416(7)
C(1)	0.754(1)	–0.177(1)	0.1176(7)
C(2)	0.627(2)	–0.171(1)	0.1083(8)
C(3)	0.467(1)	–0.003(1)	0.1001(6)
C(4)	0.515(1)	0.045(1)	0.1566(6)
C(5)	0.598(1)	0.237(1)	0.1336(7)
C(6)	0.568(1)	0.248(1)	0.0671(7)
C(7)	0.806(1)	0.264(1)	0.0460(7)
C(8)	0.881(1)	0.232(1)	0.1036(6)

Table XI. Selected Positional Parameters for $[Ni(L_{S3N2})(Cl)](BPh_4)$·$(CH_3)_2CO$ (**9**)

atom	x	y	z
Ni	0.88583(9)	0.76271(7)	0.09509(4)
Cl	0.7157(2)	0.7947(2)	0.0239(1)
S(1)	0.9960(3)	0.8798(2)	0.0494(1)
S(2)	1.0653(3)	0.7318(3)	0.1625(1)
S(3)	0.9358(2)	0.6120(2)	0.04635(9)
O(1)	0.2778(6)	0.6954(7)	0.9924(3)
N(1)	0.8394(7)	0.8916(6)	0.1397(3)
N(2)	0.7778(7)	0.6652(6)	0.1331(3)
C(1)	0.892(1)	0.9862(8)	0.1240(5)
C(2a)	0.894(1)	0.999(1)	0.0651(7)
C(2b)	0.996(2)	0.983(2)	0.0977(9)
C(3)	1.146(1)	0.853(2)	0.0877(5)
C(4)	1.175(1)	0.799(1)	0.1271(9)
C(5)	1.097(1)	0.600(1)	0.1513(4)
C(6)	1.0732(9)	0.5667(8)	0.0889(5)
C(7)	0.825(1)	0.5323(8)	0.0682(4)
C(8)	0.799(1)	0.5545(8)	0.1267(5)

(27) Drew, M. G. B.; Rice, D. A.; Richards, K. M. *J. Chem. Soc., Dalton Trans.* **1980**, 2503.

Table XII. Selected Bond Distances (Å) and Angles (deg) for Compounds **7–9**

	$[Ni(L_{S3N2})(py)](BPh_4)_2$ (**7**)		
Ni–S(1)	2.457(6)	S(3)–C(7)	1.78(3)
Ni–S(2)	2.459(6)	C(1)–C(2)	1.54(3)
Ni–S(3)	2.428(6)	C(7)–C(8)	1.52(3)
Ni–N(1)	2.09(2)	N(1)–C(1)	1.49(3)
Ni–N(2)	2.05(2)	N(2)–C(8)	1.45(3)
Ni–N(3)	2.12(1)	N(3)–C(11)	1.26(2)
S(1)–C(2)	1.78(2)	N(3)–C(15)	1.36(2)
S(1)–C(3)	1.81(2)	C(11)–C(12)	1.43(3)
S(2)–C(4)	1.74(2)	C(12)–C(13)	1.37(3)
S(2)–C(5)	1.78(2)	C(13)–C(14)	1.31(3)
S(3)–C(6)	1.82(2)	C(14)–C(15)	1.43(3)
N(3)–Ni–S(1)	90.0(4)	S(3)–Ni–N(2)	86.1(5)
N(3)–Ni–S(2)	175.3(4)	N(1)–Ni–N(2)	92.5(7)
N(3)–Ni–S(3)	91.6(4)	Ni–S(1)–C(2)	97.7(7)
N(3)–Ni–N(1)	91.7(6)	Ni–S(1)–C(3)	103.7(7)
N(3)–Ni–N(2)	89.8(6)	C(2)–S(1)–C(3)	101.0(1)
S(1)–Ni–S(2)	86.2(2)	Ni–S(2)–C(5)	104.9(7)
S(1)–Ni–S(3)	97.3(2)	Ni–S(2)–C(4)	103.1(7)
S(1)–Ni–N(1)	84.1(4)	C(4)–S(2)–C(5)	101.0(1)
S(1)–Ni–N(2)	176.6(5)	Ni–S(3)–C(6)	102.2(6)
S(2)–Ni–N(1)	90.6(5)	Ni–S(3)–C(7)	94.7(8)
S(2)–Ni–N(2)	94.2(5)	C(6)–S(3)–C(7)	103(1)
N(1)–Ni–N(2)	92.5(7)	Ni–N(3)–C(11)	122(1)
S(2)–Ni–S(3)	86.2(3)	Ni–N(3)–C(15)	119(1)
S(3)–Ni–N(1)	176.4(5)		
	$[Ni(L_{S3N2})(N_3)](BPh_4)\cdot MeCN$ (**8**)		
Ni–S(1)	2.405(3)	S(2)–C(5)	1.80(1)
Ni–S(2)	2.477(3)	S(3)–C(6)	1.80(1)
Ni–S(3)	2.426(4)	S(3)–C(7)	1.81(1)
Ni–N(1)	2.128(9)	N(1)–C(1)	1.47(2)
Ni–N(2)	2.091(9)	N(2)–C(8)	1.47(2)
Ni–N(3)	2.068(9)	C(7)–C(8)	1.51(2)
S(1)–C(2)	1.84(2)	C(1)–C(2)	1.44(2)
S(1)–C(3)	1.86(1)	N(3)–N(4)	1.17(1)
S(2)–C(4)	1.77(1)	N(4)–N(5)	1.15(1)
N(3)–Ni–S(1)	85.9(3)	S(3)–Ni–N(2)	86.0(2)
N(3)–Ni–S(2)	168.4(4)	N(1)–Ni–N(2)	89.8(4)
N(3)–Ni–S(3)	88.6(4)	Ni–S(1)–C(2)	96.7(6)
N(3)–Ni–N(1)	91.7(4)	Ni–S(1)–C(3)	103.2(3)
N(3)–Ni–N(2)	93.1(4)	C(2)–S(1)–C(3)	101.4(8)
S(1)–Ni–S(2)	85.5(1)	Ni–S(2)–C(5)	104.4(5)
S(1)–Ni–S(3)	98.1(1)	Ni–S(2)–C(4)	105.5(5)
S(1)–Ni–N(1)	86.2(4)	C(4)–S(2)–C(5)	102.7(6)
S(1)–Ni–N(2)	175.8(2)	Ni–S(3)–C(6)	105.7(5)
S(2)–Ni–N(1)	95.5(2)	Ni–S(3)–C(7)	95.5(4)
S(2)–Ni–N(2)	96.1(3)	C(6)–S(3)–C(7)	105.5(6)
S(2)–Ni–S(3)	84.9(1)	Ni–N(3)–N(4)	127.6(8)
S(3)–Ni–N(1)	175.7(3)	N(3)–N(4)–N(5)	176.0(1)
	$[Ni(L_{S3N2})(Cl)](BPh_4)\cdot(CH_3)_2C(O)$ (**9**)		
Ni–S(1)	2.385(2)	S(2)–C(4)	1.87(2)
Ni–S(2)	2.417(2)	S(3)–C(5)	1.786(9)
Ni–S(3)	2.414(2)	S(3)–C(6)	1.822(7)
Ni–N(1)	2.116(5)	S(3)–C(7)	1.807(8)
Ni–N(2)	2.107(5)	N(1)–C(1)	1.460(9)
Ni–Cl	2.390(2)	N(2)–C(8)	1.481(9)
S(1)–C(2a)	2.03(1)	C(1)–C(2a)	1.42(1)
S(1)–C(2b)	1.78(2)	C(1)–C(2b)	1.46(2)
S(2)–C(3)	1.87(2)	C(7)–C(8)	1.51(1)
Cl–Ni–S(1)	90.24(8)	S(3)–Ni–N(2)	85.9(2)
Cl–Ni–S(2)	176.40(8)	N(1)–Ni–N(2)	92.2(2)
Cl–Ni–S(3)	92.34(7)	Ni–S(1)–C(2a)	91.6(4)
Cl–Ni–N(1)	88.0(2)	Ni–S(1)–C(2b)	97.3(6)
Cl–Ni–N(2)	86.2(2)	Ni–S(1)–C(3)	100.7(5)
S(1)–Ni–S(2)	86.8(1)	C(2a)–S(1)–C(3)	125.8(7)
S(1)–Ni–S(3)	96.16(7)	C(2b)–S(1)–C(3)	86.5(8)
S(1)–Ni–N(1)	85.8(2)	Ni–S(2)–C(5)	103.6(3)
S(1)–Ni–N(2)	176.0(2)	Ni–S(2)–C(4)	101.1(5)
S(2)–Ni–N(1)	93.8(2)	C(4)–S(2)–C(5)	102.2(4)
S(2)–Ni–N(2)	96.9(2)	Ni–S(3)–C(6)	105.1(3)
S(2)–Ni–S(3)	85.98(7)	Ni–S(3)–C(7)	94.8(2)
S(3)–Ni–N(1)	178.1(1)	C(6)–S(3)–C(7)	104.3(4)

distance for the thioether which is trans to the Cl^- in structure **2** (2.455(2) Å) falls outside the normal range (2.38–2.43 Å) for 6-coordinate Ni–S(thioether) distances,[28] is 0.018 Å longer than that (2.437(8) Å) which is trans to the Br^- in structure **4** and 0.039 Å longer than that (Ni–S(2) = 2.4158(9) Å) which is trans to the MeCN in structure **1**. The mean equatorial Ni–S distances in structures **1** (2.42(2) Å) and **2** (2.406(5) Å) fall in the normal range for Ni(II)–thioether complexes.[28] Examples of homoleptic Ni(II) thioether complexes include $[Ni^{II}(TTCN)_2](BF_4)_2$,[28a] $[Ni(24S_6)]^{2+}$,[28b] and $Ni([18]\text{-ane}S_6)]^{2+}$.[28c] Examples of mixed N/S(thioether) Ni(II) complexes include $[Ni(dsbd)](BF_4)_2$,[28d] $[Ni(L_1)(ClO_4)]^+$ (**5**; L_1 = 15-thia-1,5,8,11-tetraazabicyclo-[10.5.2]nonadecane),[28e] $[Ni([9]\text{-ane}N_2S)_2]^{2+}$,[28f,g] and $[Ni([9]\text{-ane}NS_2)_2]^{2+}$.[28h] Like **1** and **2**, all of these complexes contain a 6-coordinate Ni ion. However, in contrast to structures **1** and **2**, which contain labile Cl^- and MeCN, respectively, all but one of these complexes, **5**, are coordinatively saturated and lack labile binding sites. Complex **5** contains a weakly-bound ClO_4^- ion which could conceivably be displaced by incoming ligands. The acetonitrile solvent molecule in structure **1** (Ni–N(MeCN) = 2.077(3) Å) is bound in an end-on, slightly nonlinear, fashion (Ni–N(3)–C(9) = 168.7(3)), with an unexceptional[29] C(9)–N(3) distance (1.111(4) Å). This type of distortion from linearity is commonly observed when MeCN is coordinated to a transition metal.[29b]

The Ni ion in **3** is ligated by two thiolate-type sulfurs (S(1), S(5)) and three thioether-type sulfurs (S(2), S(3), S(4)) in an elongated square pyramidal geometry. This type of mononuclear structure is rare in Ni–thiolate chemistry. The only other examples of structurally characterized mononuclear 5-coordinate Ni thiolates are square pyramidal $[Ni(TIM)(S\text{-}p\text{-}C_6H_4Cl)]^+$ [30] and trigonal bipyramidal $Ni(terpy)(S\text{-}2,4,6\text{-}(i\text{-}Pr)_3C_6H_2)_2$,[7b] Ni(DAPA)$(SPh)_2$,[31] and $NiL_{S2(Me)N3(Pr)}$.[12] The majority of Ni thiolates are oligomeric,[32] and isolation of mononuclear structures usually requires that rigid,[7c,12] electron-withdrawing,[7a] or aromatic[7b,31,33] thiolates be used. The mean $Ni\text{–}S_{thiolate}$ distance in **3** (2.19(2) Å) falls at the long end of the range observed for 4-coordinate square planar Ni thiolate complexes (2.14–2.20 Å)[7] and is noticeably shorter than that which is found in either 5-coordinate (range = 2.26–2.45 Å)[7b,12,15] or 6-coordinate (range = 2.42–2.53 Å) Ni thiolate complexes.[7e] The mean equatorial $Ni\text{–}S_{thioether}$ distance in **3** (2.21(1) Å) is considerably shorter than that which is typically found (2.38–2.43 Å) in Ni–thioether complexes, including structures **1** (2.42(2) Å) and **2** (2.406(5) Å). This distance is, however, similar to that found in the 4-coordinate thioether complex $[Ni(Me_2BME\text{-}DACO)]^{2+}$ (**6**;

(28) (a) Setzer, W. N.; Ogle, C. A.; Wilson, G. S.; Glass, R. S. *Inorg. Chem.* **1983**, *22*, 266. (b) $24S_6$ = hexathia-24-crown-6. Rawle, S. C.; Hartman, J. R.; Watkin, D. J.; Cooper, S. R. *J. Chem. Soc., Chem. Commun.* **1986**, 1083. (c) $[18]\text{-ane}S_6$ = 1,4,7,10,13,16-hexathiacyclooctadecane. Hintza, E. J.; Hartman, J. R.; Cooper, S. R.; *J. Am. Chem. Soc.* **1983**, *105*, 3738. d) dsbd = 1,12-bis(3,5-dimethylpyrazol-1-yl)-2,11-diaza-5,8-dithiadodecane. Paap, F.; Dreissen, W. L.; Reedijk, J.; Spek, A. L. *Inorg. Chim. Acta* **1988**, *150*, 57. (e) Fortier, D. G.; McAuley, A. *Inorg. Chem.* **1989**, *28*, 655. (f) $[9]\text{-ane}N_2S$ = 1-thia-4,7-diazacyclononane. Hart, S. M.; Boeyens, J. C. A.; Michael, J. P.; Hancock, R. D. *J. Chem. Soc., Dalton Trans.* **1983**, 1601. (g) Boeyens, J. C. A.; Dobson, S. M.; Hancock, R. D. J. *Inorg. Chem.* **1985**, *24*, 3073. (h) $[9]\text{-ane}NS_2$ = 7-aza-1,4-dithiacyclononane. McAuley, A.; Subramanian, S. *Inorg. Chem.* **1990**, *29*, 2830.

(29) (a) Structure of free MeCN: Danford, M. D.; Livingston, R. L. *J. Am. Chem. Soc.* **1955**, *77*, 2944. (b) Examples of structures containing MeCN coordinated to a transition metal: Capelle, B.; Beauchamp, A. L.; Dartiguenave, M.; Dartiguenave,Y.; Klein, H.-F. *J. Am. Chem. Soc.* **1982**, *104*, 3891. (c) Allison, J. D.; Fanwick, P. E.; Walton, R. A. *Organometallics* **1984**, *3*, 1515. (d) Swanson, B.; Shriver, D. F.; Ibers, J. A. *Inorg. Chem.* **1969**, *8*, 2182.

(30) TIM = 2,3,9,10-tetramethyl-1,4,8,11-tetraazacyclotetradeca-1,3,8,10-tetraene. Wilker, J. J.; Gelasco, A.; Pressler, M. A.; Day, R. O.; Maroney, M. J. *J. Am. Chem. Soc.* **1991**, *113*, 6342.

(31) DAPA = 2,6-bis[(1-phenylimino)ethyl]pyridine. Baidya, N.; Olmstead, M.; Mascharak, P. K *J. Am. Chem. Soc.* **1992**, *114*, 9666.

(32) For examples see: (a) Krueger, T.; Krebs, B.; Henkel, G. *Angew. Chem.* **1992**, *104*, 71. (b) Yamamura, T. *Bull. Chem. Soc. Jpn.* **1988**, *61*, 1975. (c) Koo, B.-K.; Block, E.; Kang, H.; Liu, S.; Zubieta, J. *Polyhedron* **1988**, *7*, 1397. (d) Dance, I. G. *Polyhedron* **1987**, *5*, 1037. (e) Tremel, W.; Kriege, M.; Krebs, B.; Henkel, G. *Inorg. Chem.* **1988**, *27*, 3886.

(33) Rosenfield, S. G.; Armstrong, W. H.; Mascharak, P. K. *Inorg. Chem.* **1986**, *25*, 3014.

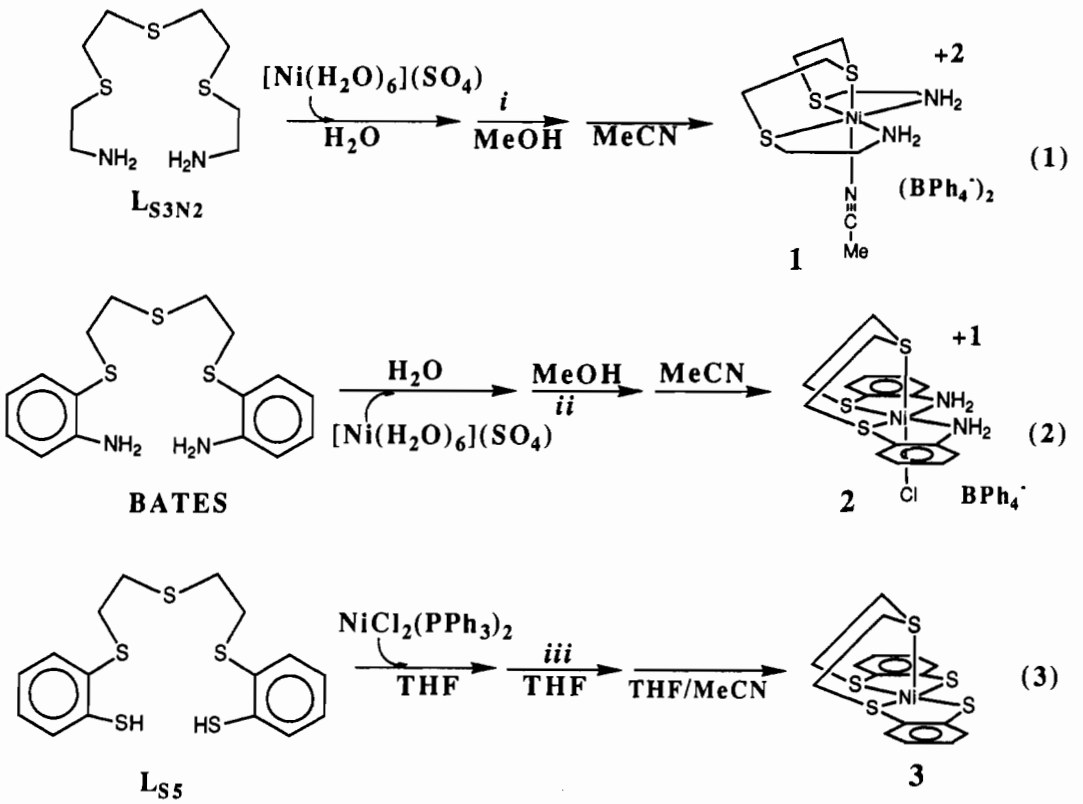

Figure 1. Synthesis of structurally-related nickel complexes **1**–**3**. Conditions: (i) $BaCl_2 + 2NaBPh_4 \rightarrow 2NaCl + BaSO_4$; (ii) $BaCl_2 + NaBPh_4 \rightarrow NaCl + BaSO_4$; (iii) $2NaOMe \rightarrow 2MeOH + 2NaCl + 2PPh_3$.

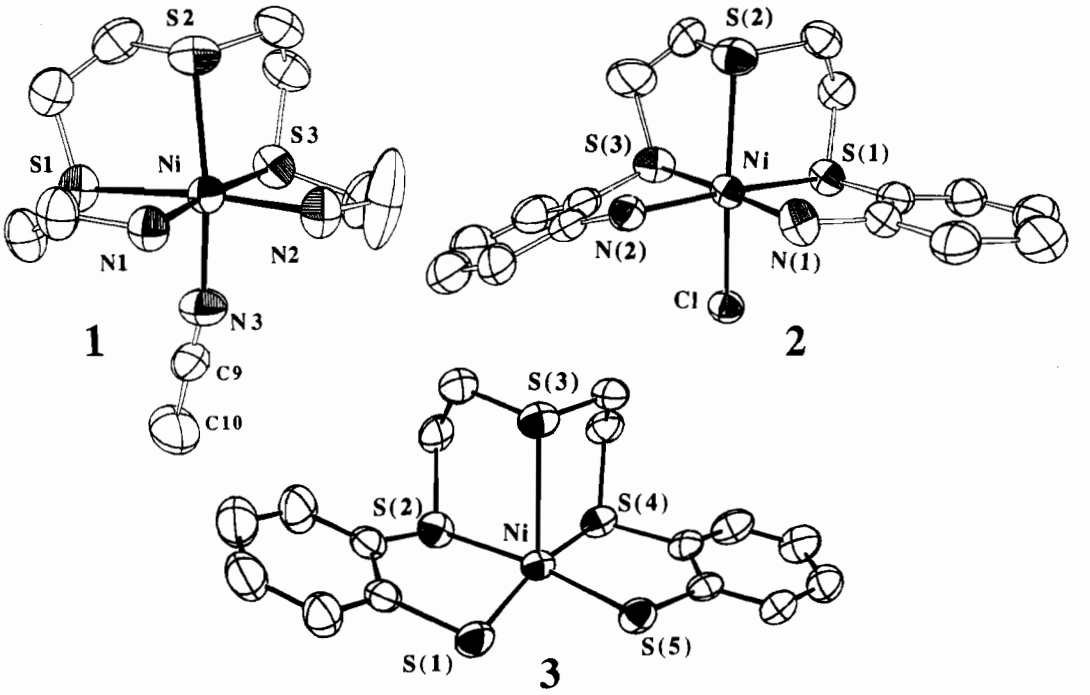

Figure 2. ORTEP plots of $[Ni(L_{S3N2})(MeCN)]^{2+}$ (**1**), $[Ni(BATES)(Cl)]^{+}$ (**2**), and $Ni(L_{S5})$ (**3**), showing 50% probability ellipsoids and atom-labeling schemes. H atoms have been omitted for clarity.

2.208(5) Å).[78] In both of these complexes, **3** and **6**, the short equatorial Ni–$S_{thioether}$ distances are probably a consequence of the low coordination number (CN = 4) and resultant diamagnetic ($S = 0$) spin state. The majority of Ni–thioether complexes are 6-coordinate (CN = 6) and high-spin (S = 1), with an occupied antibonding $d_{x^2-y^2}$ orbital which results in longer Ni–S bonds. One cannot rule out, however, the possibility that ligand constraints are responsible for the short equatorial Ni–$S_{thioether}$ distances in **3** and **6**. In contrast to what one might expect, the Ni–$S_{thiolate}$ distances in **3** (Ni–$(S1,S5)_{av}$ = 2.19(2) Å) are equivalent to the equatorial Ni–$S_{thioether}$ distances (Ni–$(S2,S4)_{av}$ = 2.21(1) Å). These results suggest that, in hydrogenase, Ni–S distances obtained from EXAFS may not differentiate a biological thioether ligand S-Met from a biological thiolate ligand S-Cys. A slightly less precise structure of **3**, in which the Ni–$S_{thioether}$ distances were described as being slightly longer than the Ni–$S_{thiolate}$ distances, has been previously reported.[26]

The L_{S5} ligand in **3** adopts a conformation which pulls the S(3) thioether atom, which is trans to the "vacant" site, back slightly so that it does not sit directly over the metal ion. This is illustrated

by the S(3)–Ni–S(1,5) angles (102.12(6) and 105.90(7)°) which deviate from the 90° angle expected for an ideal square pyramidal structure. These angles are closer to 90° in structures **1** and **2**; S(2)–Ni–N(1,2) = 96.09(7) and 99.40(8)° in **1** and 94.0(1) and 96.9(1)° in **2**. The unique Ni–S(3) bond distance in structure **3** (Ni–S(3) = 2.747(2) Å) is 0.292 Å longer than the Ni–S(2) distance (2.455(2) Å) for the thioether trans to the Cl^- in structure **2** and 0.331 Å longer than that (Ni–S(2) = 2.4158(9) Å) which is trans to the MeCN in structure **1**, and 0.32 Å longer than the sum of their covalent radii (2.43 Å), and 1.05 Å shorter than the sum of their van der Waals radii.[34] This is not surprising, given the fact that the antibonding $(d_{z^2})^*$ orbital, which is pointing toward S(3), is doubly populated in **3**. The Ni ion in **3** is displaced 0.155 Å out of the S(1)S(2)S(4)S(5) plane toward S(3), indicating that there is some sort of interaction between them. Long "apical" Ni–$S_{thioether}$ distances have also been observed in dimeric square pyramidal structures such as Ni_2L_2 (Ni–S = 2.797Å; L = *N*-[2-(2-pyridyl)ethyl]-*N*-[2-(methylthio)ethyl]-2-aminoethanethiolate)[35] and $Ni_2L'_2$ (Ni–S = 2.575(2) Å; L' = 2-[(*RS*)-1-[(*SR*)-(2-((2-hydroxybenzylidene)amino)ethyl)amino]-2-(phenylthio)ethyl]phenolate).[36] Recent EXAFS studies[37] indicate that there may be a similar long Ni–S interaction (~2.4–2.6 Å) present in H_2-ase.

Physical Properties and Reactivities of 1–3. Although redox changes (Ni(III) → Ni(II) and/or Ni(II) → Ni(I)) appear to play an important role in the mechanism of H_2-ase, none of the complexes examined in this paper display reversible redox processes in solution. Reduction of thiolate-ligated complex **3** does, however, afford a 19e⁻ Ni(I) species that displays reactivity properties similar to those of the Ni-containing enzyme methyl coenzyme M reductase.[38] The precursor to this reaction is observed in the quasi-reversible (ΔE_p = 150 mV, $i_a/i_c \sim 1.0$, scan rate = 100 mV/s) reduction wave (–1.16V vs SCE) which complex **3** displays in DMF solutions. Amine-ligated **1** displays an irreversible oxidation wave at $E_{1/2}$ = +0.96 V (vs SCE) and an irreversible reduction wave at $E_{1/2}$ = –0.85 V in MeCN. Complex **2** displays only an irreversible reduction wave at –0.87 V vs SCE in MeCN.

The 6-coordinate structures of both complexes **1** and **2** persist in solution as demonstrated by their electronic spectral properties (TableVI). Electronic spectra of **1** and **2** display the d–d transitions ($\nu_1(\Delta_0) = {}^3T_{2g} \leftarrow {}^3A_{2g}$, $\nu_2 = {}^3T_{1g(F)} \leftarrow {}^3A_{2g}$, $\nu_3 = {}^3T_{1g(P)} \leftarrow {}^3A_{2g}$) expected under approximate octahedral symmetry. Shoulder features are present in the 920–1020-nm region due to the lowered symmetry ($\leq C_s$). The electronic spectrum of **1** is solvent-dependent, and $\nu_1(\Delta_0)$ red-shifts upon dissolution in O-containing solvents such as DMF or acetone (*vide infra*). The electronic spectrum of **2** is essentially the same in MeCN and acetone, indicating that the Cl^- ion bound to the sixth site of **2** is not replaced by these coordinating solvents.

The 5-coordinate structure of **3** persists in all but the most strongly coordinating solvent, pyridine, as demonstrated by its electronic spectral (Table VI), ^{1}H NMR (Table VII), and magnetic properties. The UV/vis/near-IR spectra of **3** are nearly identical in THF, DMF, and CH_2Cl_2, and display two d–d bands in the region 550–700 nm with extinction coefficients consistent with a 5-coordinate structure. In pyridine a new, lower energy, band appears at 970 nm. Magnetic susceptibility data indicate that **3** is diamagnetic, both in the solid state and in DMF, THF, and CH_2Cl_2 solutions, but paramagnetic (μ_{eff}(py, 249 K)) = 0.96 μ_B) in pyridine. Thus, **3** appears to remain 5-coordinate, in coordinating solvents DMF and THF and in CH_2Cl_2, and partially converts to a 6-coordinate structure in pyridine. Temperature-dependent UV/vis/near-IR (Table VI) and ^{1}H NMR (Table VII) data indicate that an equilibrium mixture, consisting of **3** and a green paramagnetic solvent-ligated derivative, [Ni(L_{S5})(py)], forms in neat pyridine. ^{1}H NMR peaks of **3** in neat py-d_5 (Table VII) are paramagnetically shifted most dramatically at low temperatures (e.g., at 248 K: δ 42.0, 29.8, 25.5, 16.1) and gradually move toward the diamagnetic region as the temperature is raised. As the temperature is lowered, UV/vis/near-IR bands in the region 550–600 nm shift to lower energies (Table VI), the extinction coefficients drop closer to that expected for a 6-coordinate structure, and a low-energy band grows in at 970 nm. High temperatures clearly favor the diamagnetic 5-coordinate structure Ni(L_{S5}), whereas low temperatures appear to favor a paramagnetic 6-coordinate structure, possibly [Ni(L_{S5})(py)]. The amine-ligated complexes **1** and **2**, on the other hand, remain paramagnetic at all temperatures examined. Complex **1** has magnetic moments of μ_{eff}(MeCN) = 2.85 μ_B in solution and μ_{eff}(24 °C) = 2.90 μ_B in the solid state, which is consistent with an S = 1 ground state. Complex **2** displays similar magnetic properties with μ_{eff}(MeCN) = 3.06 μ_B in solution and μ_{eff} = 3.18 μ_B in the solid state.

Although it remains 6-coordinate, the Ni-bound MeCN solvent molecule of **1** is exchangeable and is reversibly displaced by weaker coordinating solvents (e.g., DMSO, $(CH_3)_2C(O)$, H_2O, and MeOH) and irreversibly displaced by anionic ligands. Solvent binding is accompanied by red shifts in the UV/vis/near-IR spectrum. The influence of solvents on the energy of ν_1, which corresponds to Δ_0 for a d^8 octahedral complex, follows the expected order (MeCN (Δ_0 = 11 310 cm^{-1}) > DMF (Δ_0 = 9862 cm^{-1}) ~ $Me_2C(O)$ (Δ_0 = 9785 cm^{-1})), with N-containing MeCN producing a stronger ligand field than O-containing acetone, for example. Additional evidence for solvent binding is provided by the appearance of new bands in the solid-state IR spectra, which correspond to bound solvent stretches (e.g., $\nu_{C=O}$ or $\nu_{S=O}$). For example if **1** is repeatedly dissolved in acetone and bulk solvent removed in vacuo, then the isolated compound displays a new $\nu_{C=O}$ stretch in the IR(KBr), which is shifted (–11 cm^{-1}) relative to that of free acetone ($\nu_{C=O}$ = 1713 cm^{-1}), and the ν_{CN} stretch (2249 cm^{-1}) of the parent MeCN-ligated complex disappears. Solvent-ligated derivatives of **1**, [Ni(L_{S3N2})(solv)]$^{2+}$ (solv = DMSO, $(CH_3)_2C(O)$, H_2O, MeOH), exist in equilibrium with [Ni(L_{S3N2})(MeCN)]$^{2+}$ (**1**), and mixtures are obtained unless care is taken to remove all of the MeCN. Water appears to bind most weakly to **1** ([Ni(L_{S3N2})(H_2O)](SO_4) (**1b**)) and can be removed by slightly heating purple solid **1b** under vacuum. This converts **1b** to a green, presumably 5-coordinate solid, possibly [Ni(L_{S3N2})](SO_4), which slowly picks up moisture from the air and converts back to the purple water-ligated compound. This process can be repeated with no noticeable decomposition.

Reaction of **2** with $NaBH_4$ in MeCN-d_3 at –42 °C results in an immediate color change from lavender to blue and affords a thermally unstable species **10**, which decomposes upon warming to form free ligand, Ni mirror, a black solid (nickel boride),[24] and H_2 gas. The thermally unstable blue species **10** behaves like a Ni–H in terms of its reactivity. Addition of olefins, such as styrene or cyclohexene, to NMR tubes containing blue, homogeneous solutions of "Ni–H" (**10**) at –42 °C, followed by warming to room temperature, results in the formation of the corresponding hydrogenated products, ethylbenzene (75% detected by ^{1}H NMR) and cyclohexane (62% detected by ^{1}H NMR). $CDCl_3$ is converted to $CHDCl_2$ (53% detected by ^{1}H NMR)—a reaction which is commonly used as a test for the presence of M–H compounds.[39] Hg has no effect on these reactions, thus ruling out a heterogeneous reaction involving colloidal Ni^0.[40] If solutions are allowed to warm to room temperature prior to the addition of olefin or $CDCl_3$, then no hydrogenated products or $CHDCl_2$ is detected. This also

(34) Pauling, L. *The Nature of the Chemical Bond*, 3rd ed.; Cornell University Press: Ithaca, NY, 1960; p 260.
(35) Handa, M.; Mikuriya, M.; Okawa, H.; Kida, S. *Chem. Lett.* **1988**, 1555.
(36) Berkessel, A. *Bioorg. Chem.* **1991**, *19*, 101.
(37) (a) Scott, R. A. Personal communication. (b) Whitehead, J. P.; Colpas, G. J.; Bagyinka, C.; Maroney, M. J. *J. Am. Chem. Soc.* **1991**, *113*, 6288.
(38) Cha, M.; Shoner, S. C.; Kovacs, J. A. *Inorg. Chem.* **1993**, *32*, 1860.
(39) Collman, J. P.; Hegedus, L. S.; Norton, J. R.; Finke, R. G. *Principles and Applications of Organotransition Metal Chemistry*; University Science Books: Mill Valley, CA, 1987.
(40) Anton, D. R.; Crabtree, R. H. *Organometallics* **1983**, *2*, 855.

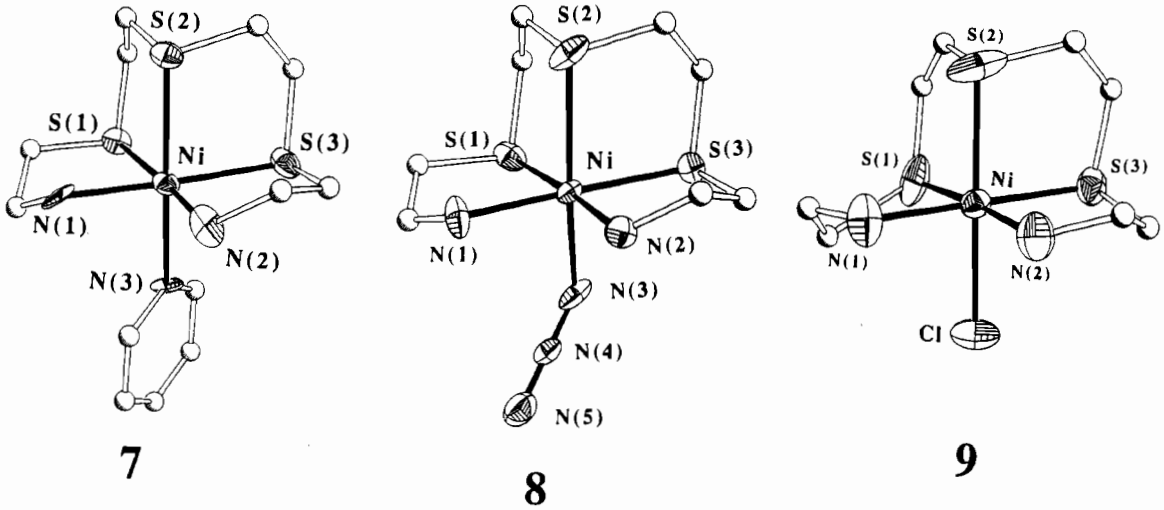

Figure 3. ORTEP plots of $[Ni(L_{S3N2})(py)]^{2+}$ (**7**), $[Ni(L_{S3N2})(N_3)]^{+}$ (**8**), and $[Ni(L_{S3N2})(Cl)]^{+}$ (**9**) showing atom-labeling schemes and 50% probability ellipsoids for Ni, S, and N. Since there was considerable disorder in structures **7** and **9**, thermal ellipsoids were not included for the carbons in all three structures. H atoms have been omitted for clarity.

suggests that the reactions are not heterogeneously promoted by the thermal decomposition products H_2 + Ni^0. If the reactions are monitored by ^1H NMR, then, although the reactant concentration decreases at −20 °C, no products are observed until the solution is allowed to warm to room temperature. This would seem to indicate that a paramagnetic Ni-bound form of the product (e.g., a nickel alkyl), which is not detectable by ^1H NMR, forms at low temperature and that product (e.g., alkane) is not released until the temperature is raised. In any case, the observed reactivity (i.e., olefin hydrogenation and H atom transfer to $CHCl_3$) of **2** and $NaBH_4$ provides indirect evidence for the formation of a thermally unstable Ni–H species. It is possible that a Ni–borohydride species is forming, however, we know of no examples of homogeneous transition metal borohydrides that will promote the observed reactions. The BATES ligand does not appear to be necessary for these reactions to occur, however; reaction of $NiCl_2$ with $NaBH_4$ also forms a species which will hydrogenate olefins. Nickel borides, formed from $NiCl_2$ and $NaBH_4$, have been shown to hydrogenate olefins in a heterogeneous reaction under similar conditions;[24] however, in the presence of coordinating solvents (e.g., DMF or MeCN) or complexing ligands (e.g., en, NH_3, or cyclic tetraamines), the active species are believed to be homogeneous and Ni–H's of undetermined nature.[41] Whether these species are coordinated by solvent or complexed by the sulfur-containing BATES ligand, these results do indicate that a Ni–H species is capable of forming in the absence of Cp, CO, and/or PR_3 ligands, which are unlikely to be present in hydrogenase. Mascharak and co-workers have also shown, by EPR, that a Ni(I)–H species, $[Ni(terpy)(SR)_2(H)]^{2-}$, will form in a reaction between $NaBH_4$ and Ni(terpy)(S-2,4,6-(*i*-$Pr)_3C_6H_2)_2$.[7b] Holm and co-workers have shown that a stable thioether-ligated Ni–H complex $[Ni(NS_3^{tBu})(H)]^{+}$ forms at room temperature in THF solution.[42] The presence of a hydride was confirmed by IR and ^1H NMR and by its reactivity with ethylene, to form a Ni–Et derivative, and halogenated hydrocarbons, to form a Ni–Cl derivative. Crabtree and co-workers recently reported a labile, sulfur-ligated Ni(II) complex which will promote H_2/D^{+} exchange[43] and a N-containing macrocyclic Ni complex which will electrocatalytically reduce protons to H_2.[44] Although they are not directly observed, both of these reactions probably proceed through a Ni–H intermediate. In this study, we have found that complex **1** will also form a Ni–H which behaves analogously to the Ni–H derivative of **2**. Reaction of $NaBH_4$ with **3**, on the other hand, results in C–S bond cleavage.[14c,38]

Table XIII. Comparative Structural Parameters for $[Ni(L_{S3N2})(L)]^{n+}$ (n = 1, 2; L = MeCN, py, N_3^-, Cl^-, Br^-)

	MeCN (**1**)	py (**7**)	N_3^- (**8**)	Cl^- (**9**)	Br^- (**4**)[a]
Ni–S(1)	2.439(1)	2.457(6)	2.405(3)	2.385(2)	2.393(6)
Ni–S(2)	2.4158(9)	2.459(6)	2.477(3)	2.417(2)	2.437(8)
Ni–S(3)	2.4057(9)	2.428(6)	2.426(4)	2.414(2)	2.393(6)
Ni–N(1)	2.077(2)	2.09(2)	2.128(9)	2.116(5)	2.074(17)
Ni–N(2)	2.097(3)	2.05(2)	2.091(9)	2.107(5)	2.074(17)
Ni–N(3)	2.078(3)	2.12(1)	2.068(9)		
Ni–X[b]				2.390(2)	2.578(5)

[a] Parameters taken from: Drew, M. G. B.; Rice, D. A.; Richards, K. M. *J. Chem. Soc., Dalton Trans.* **1980**, 2503. Distances quoted correspond not to the atom labels given in the above reference but to those used in this paper. [b] X = Cl, Br.

The most stable derivatives of **1** are those which contain either pyridine or anionic ligands, such as Cl^- and N_3^-, bound to the sixth coordination site. Single-crystalline samples of $[Ni(L_{S3N2})(py)](BPh_4)_2$ (**7**), $[Ni(L_{S3N2})(N_3)](BPh_4)$ (**8**), and $[Ni(L_{S3N2})(Cl)](BPh_4)$ (**9**) were obtained as described in the Experimental Section.

Structures of 7–9. ORTEP diagrams of dicationic $[Ni(L_{S3N2})(py)]^{2+}$ (**7**) and monocationic $[Ni(L_{S3N2})(N_3)]^{+}$ (**8**) and $[Ni(L_{S3N2})(Cl)]^{+}$ (**9**) are shown in Figure 3. Selected interatomic distances and angles are collected in Table XII. Structures **7** and **9** were poor quality due to the presence of disordered solvate molecules, which either could not be identified or could not be modeled. Two of the methylene carbons C(2) and C(3) in the trithioether "backbone" of **9** were also disordered, and this could only be modeled for one of them (C(2)). Despite these disorder problems, however, the connectivity and bond distances of the Ni cations were determined with enough precision to allow a comparison with the parent molecule $[Ni(L_{S3N2})(MeCN)](BPh_4)_2$ (**1**). Structural parameters are compared for $[Ni(L_{S3N2})(L)]^{n+}$ (n = 1, 2; L = MeCN (**1**), py (**7**), N_3^- (**8**), Cl^- (**9**), Br^- (**4**)) in Table XIII. Like structure **1**, structures, **7–9** are all distorted from C_s symmetry. With the exception of the Ni–S(2) distance, which involves the thioether that is trans to the unique ligand L, metrical parameters for these derivatives **7–9** do not differ significantly from those of **1**. Mean Ni–S and Ni–N distances in the plane that is orthogonal to the unique ligand L only vary from 2.393(6) Å in **4** to 2.44(2) Å in **7**, and from 2.07(3) Å in **7** to 2.111(6) Å in **9**, respectively. The Ni–S(2) distance increases from 2.4158(9) Å in **1** to 2.477(3) Å in **8** and is virtually identical for structures **1** and **9**. Replacement of MeCN with chloride appears to cause the least amount of perturbation to the structure.

(41) Wade, R. C.; Holah, D. G.; Hughes, A. N.; Hui, B. C. *Catal. Rev.—Sci. Eng.* **1976**, *14*, 211.
(42) Stavropoulos, P.; Muetterties, M. C.; Carrie, M.; Holm, R. H. *J. Am. Chem. Soc.* **1991**, *113*, 8485.
(43) Zimmer, M.; Schulte, G.; Luo, X.-L.; Crabtree, R. H. *Angew. Chem., Int. Ed. Engl.* **1991**, *30*, 193.
(44) Efros, L. L.; Thorp, H. H.; Brudvig, G. W. W.; Crabtree, R. H. *Inorg. Chem.* **1992**, *31*, 1722.

Pyridine and azide binding causes slightly more significant structural changes with the trans Ni–S(2) distance, which lengthens, by 0.04 and 0.06 Å, respectively, so that they fall outside the normal range (2.38–2.43 Å). The observed angles Ni–N(3)–N(4) = 127.6(8)° and N(3)–N(4)–N(5) = 176.0(1)° in **8** are typical for azide ligands that are nonbridging.[45] Similarly, the longer N–N separation (N(3)–N(4) = 1.17(1) Å) between the middle nitrogen N(4) and the nitrogen coordinated to the metal N(3) relative to that between N(4) and the terminal nitrogen N(5) (N(4)–N(5) = 1.15(1) Å) is the usual observation for end-on-coordinated N_3^-. Ni–S(2) distances within the series $[Ni(L_{S3N2})(L)]^{n+}$ (n = 1, 2; L = MeCN (**1**), py (**7**), N_3^- (**8**), Cl^- (**9**), Br^- (**4**)) indicate that the trans influence follows the order N_3^- > py > Br^- > Cl^- ~ MeCN. Comparison of the two chloride-ligated complexes, $[Ni(L_{S3N2})(Cl)]^+$ (**9**) and $[Ni(BATES)(Cl)]^+$ (**2**), shows that the Ni–S(2) distance (2.417(2) Å in **9** vs 2.455(2) Å in **2**) reflects not only the trans influence of the opposite ligand but also ligand constraints and the ligand-field strength of the ligands in the plane orthogonal to the unique ligand L.

Comparative Properties of Amine-Ligated Complexes 1, 2, and 7–9 and Thiolate-Ligated 3. Structures **1-3** and **7-9** share a common trithioether ($S_{apical}(C_2H_4SeqR_{eq})_2$) "backbone" ($R_{eq}$ = $C_2H_4NH_2$ (**1**, **7–9**), $C_6H_4NH_2$ (**2**), and $C_6H_4S^-$ (**3**)), which is flexible enough to accommodate Ni–S_{apical} distances ranging from 2.4159(9) Å in **1** to 2.747(2) Å in **3**. The parent complex **1** and complexes **2** and **3** differ from one another in terms of their molecular charge (2+ (**1**), 1+ (**2**), 0 (**3**)) and the terminal ligating atoms (aliphatic amine (**1**) vs aromatic amine (**2**) vs aromatic thiolate (**3**)). The $-CH_2CH_2-S-CH_2CH_2-$ fragment of these ligands is also found in *macrocyclic* thioether ligands,[46] such as [18]-aneS_6,[47] [9]ane-S_3,[48] [9]-aneNS_2,[28h] and [9]-aneN_2S.[28f,g] The Ni(II) complexes derived from these *macrocyclic* ligands have been thoroughly studied and share many of the properties (e.g., spin state, coordination number, etc.) of complexes **1**, **2**, and **7-9**. However, the pentadentate nature of the BATES and L_{S3N2} ligands found in **1**, **2**, and **7-9** leaves one site available on the Ni ion for binding substrate, and the "open architecture" has allowed the series to be extended to include thiolates. Thiolates appear to have a dramatic influence on the properties of the resulting molecules. The amine-ligated complexes **1**, **2**, and **7-9** appear to have a higher affinity for axial ligands, on the bases of the fact that they preferentially form 6-coordinate structures and, consequently, at least in the case of complexes **1** and **2**, are more reactive. In contrast, the thiolate-ligated complex **3** is fairly unreactive with respect to binding axial ligands. The observed axial ligand affinity of structures **1** and **2** is not surprising on the bases of the behavior of the majority of mixed amine/thioether-ligated Ni(II) complexes.[28d-h] The observed decrease in reactivity upon substitution of terminal amines with aromatic thiolates has, however, interesting implications with respect to the Ni–binding site of hydrogenase. For complex **3**, the decreased axial ligand affinity could be attributed to either the stronger equatorial ligand field, ligand constraints, and/or the neutral molecular charge. Axial ligand binding to **3** would require a spin-state change ($S = 0 \rightarrow S = 1$) that would place an electron in the antibonding $d_{x^2-y^2}$ orbital. Unless the binding strength of the incoming axial ligand is comparable to that of the equatorial ligands, axial ligand binding would be disfavored, since it would require that the $M-L_{equatorial}$ bonds lengthen in response to the population of the antibonding $d_{x^2-y^2}$ orbital. Pyridine is the only ligand examined in this study which was strong enough to induce the required spin-state change in converting $Ni(L_{S5})$ (**3**) to $[Ni(L_{S5})(py)]$. If we assume that the Ni-binding site in hydrogenase is in any way similar to that of **3**, then these observations would seem to indicate that it would be difficult for H_2 to bind axially to the Ni ion, since H_2 is usually considered to have a binding strength which is comparable to that of H_2O[49] and therefore weaker than that of pyridine. If one were to alter the structure of **3** so that a stronger ligand (e.g., a SR^- or NH_2 in place of SR_2) were placed in the site opposite to the "vacant" site of **3**, then it is likely that the axial ligand affinity at the opposite site would increase. We are currently working on ligands which incorporate these features.

Recent magnetization[9] and MCD[2h] studies indicate that the EPR-silent form of H_2-ase contains low-spin diamagnetic Ni^{2+}. If it is assumed that the EPR-silent form being examined in these studies was the reactive form of H_2-ase, then our work, which suggests that Ni^{2+} must be high-spin in order to bind substrate, would seem to contradict these studies. One could argue, however, that the form examined by MCD and magnetization studies was not the reactive form and that the site has to be transformed somehow into a high-spin system before H_2 can bind. The fact that the enzyme can be poised in this state would imply that this is not a highly reactive species. Also, since these studies were done at low temperature, it is possible that the spin state is different (i.e., high-spin) at ambient temperature—the physiological conditions under which H_2-ases operate.

The results reported herein illustrate the influence that local coordination environment can have on a Ni ion's propensity to bind an axial ligand if it is situated in a S-rich environment resembling that of hydrogenase. In the presence of a common trithioether backbone, thiolate-type sulfur ligands were found to discourage ligand binding, whereas amine ligands favored this interaction.

Acknowledgment. Financial support from the National Institutes of Health (Grant GM45881) and the Petroleum Research Fund (Grant 22562-G5), administered by the American Chemical Society, is gratefully acknowledged. We thank Ron Stenkamp for helpful discussions and Steve Shoner for experimental assistance.

Supplementary Material Available: Tables of crystallographic data and details of data collections, atomic positional and thermal parameters, bond distances and angles, calculated hydrogen atom positional parameters, and torsional angles (54 pages). Ordering information is given on any current masthead page.

(45) For reviews of transition metal azide complexes see: (a) Dori, Z.; Ziolo, R. F. *Chem. Rev.* **1973**, *73*, 247. (b) Muller, U. *Struct. Bonding* **1973**, *14*, 141.
(46) Cooper, S. R. *Acc. Chem. Res.* **1988**, *21*, 141.
(47) Cooper, S. R.; Rawle, S. C.; Hartman, J. R.; Hintsa, E. J.; Admans, G. A. *Inorg. Chem.* **1988**, *27*, 1209.
(48) [9]ane-S_3 = 1,4,7-trithiacyclononane = TTCN. (a) Setzer, W. N.; Ogle, C. A.; Wilson, G. S.; Glass, R. S. *Inorg. Chem.* **1983**, *22*, 266. (b) Sellmann, D.; Zapf, L. J. *Organomet. Chem.* **1985**, *289*, 57.
(49) Kubas, G. J.; Burns, C. J.; Khalsa, G. R. K.; Van Der Sluys, L. S.; Kiss, G.; Hoff, C. D. *Organometallics* **1992**, *11*, 3390.